# A NUMERICAL MODEL OF THE CIRCULATION IN ÖRESUND. EVALUATION OF THE EFFECT OF A TUNNEL BETWEEN HELSINGÖR AND HELSINGBORG

by Jonny Svensson and Wayne Wilmot

SMHI Rapporter

HYDROLOGI OCH OCEANOGRAFI
Nr RHO 15 (1978)

SVERIGES METEOROLOGISKA OCH HYDROLOGISKA INSTITUT

# A NUMERICAL MODEL OF THE CIRCULATION IN ÖRESUND. EVALUATION OF THE EFFECT OF A TUNNEL BETWEEN HELSINGÖR AND HELSINGBORG

by Jonny Svensson and Wayne Wilmot

SMHI Rapporter

HYDROLOGI OCH OCEANOGRAFI
Nr RHO 15 (1978)

MODELLER AV CIRKULATIONEN I ÖRESUND. UTVÄRDERINGAR AV EFFEKTERNA AV EN TUNNEL MELLAN HELSINGBORG OCH HELSINGÖR.

SVERIGES METEOROLOGISKA OCH HYDROLOGISKA INSTITUT
Norrköping 1978

ISSN 0347-7827

CONTENTS

## INTRODUCTION

This report is to describe the application of a previously developed two-dimensional hydrodynamic numerical model (W.Wilmot 1976) to Öresund between Sweden and Denmark. The purpose of this application is to investigate the effect of a proposed tunnel connecting Helsingborg in Sweden and Helsingör in Denmark on the circulation and salinity-content of the Sound.

The model result is first compared with synoptic field data from the Sound. The effects of the proposed tunnel are investigated by comparing model results with and without the tunnel.

The tunnel between Helsingör and Helsingborg is planned to be built partly below the bottom, but partly on an artificial bank across the deeper part of the Sound. The exact position of the tunnel has not yet been decided. Among the different proposals given, this report concerns only the situation which gives the maximum change in the sectional area compared to the natural case.

Three alternative depths are given for the tunnel. The main proposal is a distance from the free surface to the roof of the tunnel of 24 m. Also the depths 28 m and 20 m can be considered.

The sill depth through Öresund into the Baltic Sea is about 8 m and the tunnel is therefore not considered to change the water exchange between the Baltic and the North Sea. However, south of the planned tunnel (see fig 1) there are areas with depths of 30 m and more. The circulation and salinity of these areas are studied in the model with various external conditons.

The same study has also been carried out in a two-layer numerical model (Danish Hydraulic Institute 1977) and to a limited extent in a channel model including an advanced turbulence description (Technical High School, Lund 1976). The ultimate result from the hydrodynamic model studies has been the basis of an ecological model and other ecological considerations (Vandkvalitetsinstitutet 1976).

ORESUND

Topography

The general topography in the model has been adapted from Swedish nautical charts and a number of more detailed maps of the area. The representation of the topography in the numerical model has been simplified somewhat since the model does not represent longitudinal scales of less the two kilometers. The region of major importance is the deep channel which runs from between Helsingör and Helsingborg, to the east of the island of Ven and ends on the east side of the Sound near Barsebäck. The maximum depth of the channel

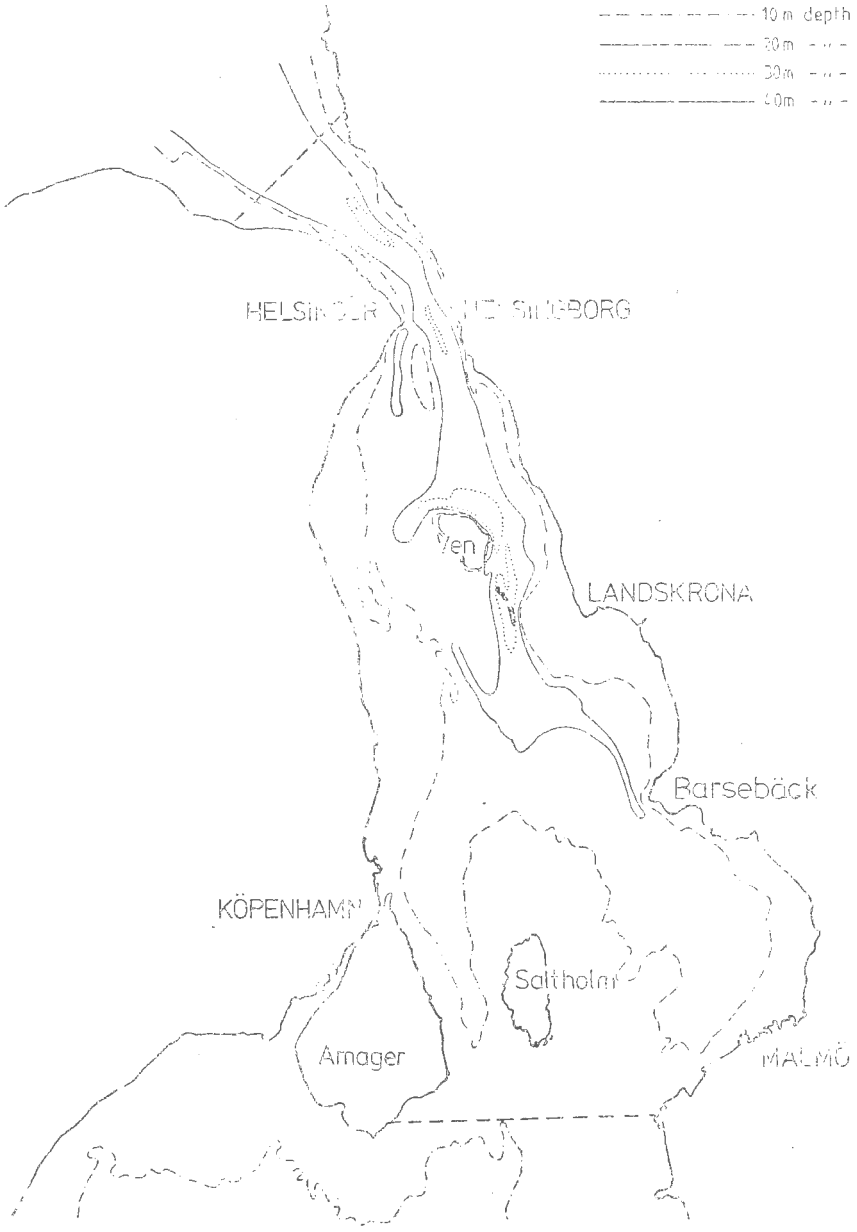


Figure 1.

is about 50 meters in an isolated depth outside Landskrona. The sill depth to this area is about 24 meters. The sill itself is a wide area on the border of Kattegatt where the depth varies between 20 and 24 meters.

The opening of the Sound into the Baltic consists of two channels: one to the east and one to the west of the island of Saltholm. The sill depths of these channels are only 8 meters.

The depth of Öresund between Helsingör and Helsingborg is at most about 30 meters. This channel is situated midway between Denmark and Sweden (see fig 1). The proposed tunnel is planned to allow a maximum depth of 24 meters in the middle of the Sound. Other depth of the tunnel are also being discucced, e.g., 28 meters.

A tunnel at a depth of 24 meters will not change the sill depth to the deeper area inside Öresund but it will very much change the sectional area where the deep water exchange takes place.

| | Total sectional area | Reduction of sectional area | Sectional area below 20 m | Reduction of sectional area |
|---|---|---|---|---|
| Without tunnel | 75 000 $m^2$ | | 13 000 $m^2$ | |
| Tunneldepth 28 m | 64 000 $m^2$ | 15 % | 6 500 $m^2$ | 50 % |
| Tunneldepth 24 m | 59 000 $m^2$ | 21 % | 2 500 $m^2$ | 81 % |

Table. Reduction of the sectional area between Helsingör and Helsingborg with different tunnel-alternatives.

The width of the channel perpendicular to the centre of the deepest part of the channel is of importance to the numerical model. Compare the model representation and the real Öresund in fig 1 and 2.

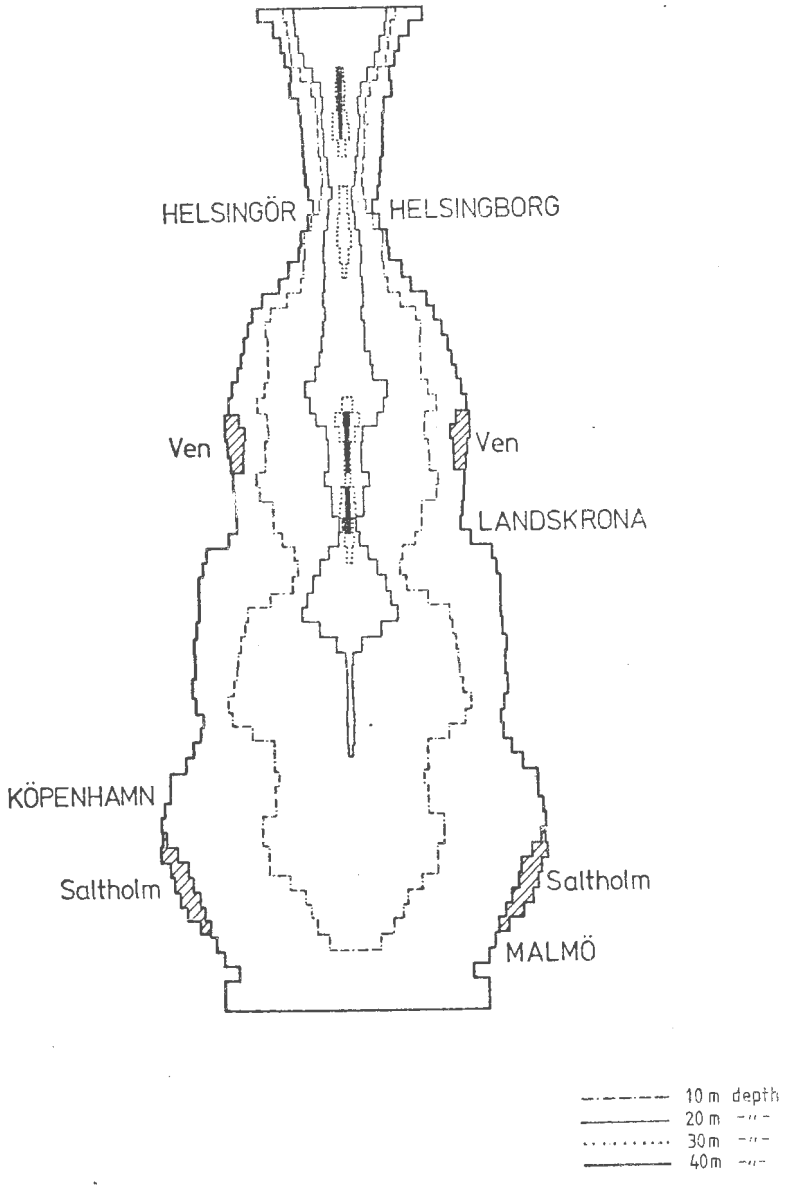


Figure 2. Modelrepresentation of Öresund

Hydrography

Öresund is part of the entrance from the North Sea into the Baltic Sea. The salinity in the surface water of the Baltic Sea is, due to runoff, low compared with that of Skagerack-Kattegatt and the North Sea. In the southern Baltic the surface salinity is close to 8 ‰. To the north of Öresund in Kattegatt the surface salinities vary, but usually are between 20 ‰ and oceanic salinity.

Fresh water amounting to approximately 450 $km^3$ per year (14 000 $m^3/s$) flows from rivers into the Baltic. This water is mixed with saline water and transported out through the Belts and Öresund. Through the mixing the outgoing volume is increased to about 900 $km^3$/year. Consequently there is a transport of salt water from the North Sea into the mixing region of about 450 $m^3$/year.

The current pattern in Öresund and the Belts is often a two layer system with an outgoing brackish water on top of an incoming salty water. There are also records of three-layer systems and of situations with an almost continous increasing salinity from the surface to the bottom. During periods with strong westerly wind the outgoing current can totaly cease and salt water penetrate into the sounds from surface to bottom.

In Öresund the bottom water in the deep area south of Ven is renewed through the channel between Helsingör and Helsingborg mainly during the stormy autumn and winter seasons. Salt intrusion during other parts of the year can also occur when the pycnocline of Kattegatt is raised enough to allow water to go over the sill (24 m). Mixing from above is also a way of renewing the deep water in the area.

The proposed tunnel will probably decrease the amount of water penetrating into the deep waters south of Ven during

the stormy season. However, it is believed that enough water will still be transported in to allow a total renewal of the whole volume of bottom water at every stormy event.

The smaller salt intrusions during the rest of the year are partly prohibited by the tunnel thereby causing a situation close to stagnation during the spring and summer. Mixing through the pycnocline can be changed if the tunnel increases or decreases the density difference between the surface and the bottom waters. A smaller density difference will thus give a more intense renewal by mixing from above.

This model study devotes ifself to the two latter problems: Inflow of salt water under calm to moderate weather conditions have been studied both with and without the tunnel. The value of the vertical mixing coefficient has been computed as a function of density stratification and wind velocities.

Water-level

The tidal range in the south part of Kattegatt is only about 12-15 cm and the tides in the Baltic are negligible. The currents in Öresund caused by tides are therefore small compared to other existing currents in the area.

Water-level changes due to wind stress and air pressure dominate in Kattegatt and the Baltic. A westerly wind will e.g. pile up water in Skagerack and Kattegatt while water is driven away from the west part of the southern Baltic. The wind effect can cause a difference of meters in the water-level between Kattegatt and the Baltic Sea.

In the modelling work the effect of water-level differences on the current (barotropic effects) has been separated from the effects of the density differences (baroclinic effects). The assumption thus made is that the baroclinic response does not alter the barotropic response. This is

generally accepted as valid in modelling. It means that the integrated transport caused by recorded water-level gradients is calculated. This transport is then fed into the baroclinic model as boundary values. The velocity resulting consists of the "known" barotropic velocities and the baroclinic response.

## PHYSICAL MODEL STRUCTURE

### Formulation philosophy

Öresund has an observed salt-heat balance characteristic of a fjord estuary (Rattray, 1967). River runoff provides a net flux of water out of the Baltic through the sill region. Brackish water flows out of the Danish Belts and Öresund, carrying salt which has been mixed upward from heavier oceanic water flowing into the Baltic at depth. The deep inflow is driven by the density difference between the oceanic water in Kattegatt and the brackish Baltic water. The density difference is maintained by sources of buoyancy: runoff and solar heating in the Baltic. The inflow is highly time dependent. This is essentially due to varying meteorological forcing, the fluctuations in the river runoff being of negligible importance. Strong southgoing currents in Öresund occur in connection with particular meteorological conditions over the North Sea - Baltic Sea region, leading to an almost complete renewal of the Öresund water. The vertical mixing in the region plays an important role in the salt balance by acting to reduce the salinity of inflowing oceanic water and to increase the salinity of the outflowing brackish water.

### Basic Approximations

The governing hydrodynamical equations express the velocity and density fields as functions of space and time. Even in their complete form they merely represent approximations to nature. Turbulence can be formally represented by an infinite set of coupled equations. It is impractical, however, to look for solutions to any but the lowest few orders of turbulent equations The turbulent equations are often avoided entirely by assuming that the turbulence acts in a way analogous to molecular processes. Turbulent diffusion is then represented as the product between an eddy coefficient and the mean gradient. The model presented here does not attempt to go beyond this simple representation of turbulence. However the vertical salt and heat diffusion coefficients are not constants but funtions of the vertical velocity differences and of the density stratification.

The scaling of the basic equations gives an idea of which processes predominate. The equation of vertical motion in estuaries can be represented quite accurately by the hydrostatic balance. That is to say that vertical momentum is unimportant.

The vertical pressure gradient adjusts itself to the density field. Furthermore, density variations are only important in the momentum balance through the horizontal pressure gradient. The density can be considered as a constant when multiplying the accelerations or friction terms (boussinesq approximation). The flow is incompressible making the velocity field non-divergent. The vertical velocity enters in order to account for divergences in the horizontal flow. Vertical flow is essential for the transport of salt, heat and horizontal momentum in estuaries.

Further simplification of the equations can be achieved by applying knowledge of estuarine circulation obtained from field observations. It is often observed in long narrow fjord type estuaries that the predominant gradients run along the channel. The cross channel gradients are much smaller. This is often due to the fact that a major source of fresh water is present at one end of the channel. Öresund is of this type. This situation allows for a reduction in the number of space coordinates. The salt and heat equations can be averaged across the channel. The momentum equations along and across the channel can be decoupled by assuming that the cross channel velocity is much smaller than the velocity along the channel. This could be viewed as a canal model in which the velocity along the channel is accelerated or decelerated by width variations.

The equations remaining, after all of the above simplifications have been made, are still non linear and quite difficult to solve analytically. The salt, heat and vorticity equations are time dependent and non linear. The continuity equation and non linear equation of state complete the set of equations to be solved.

It has been assumed that the barotropic response of the basin is independent of the internal density field. That is the water transport through Öresund due to water level changes are not influenced by the density field. The transport caused by water level changes inside the Sound is neglected.

The barotropic response is calculated in a one dimensional canal model. (Svansson, Szaron, 1975). The forcing is the measured, time dependent waterlevel difference between the north and south model boundary. The transport is modified by bottom stress.

Salt-heat conservation

The salt and heat balance equations in three dimensions can be averaged across an eatuary of width b (x,z) (Pritchard, 1958) by assuming lateral homogeneity, (figs A, B). This is equivalent to assuming that the cross estuary variations of salinity and heat are small compared to the longitudinal variations.

The boundary conditions are not obvious. There is no clear point at which the effect of the Sound on the Baltic or on the Kattegatt can be considered to end. If the observed vertical density distribution are specified, a problem occurs in the regions of outflow where the outgoing water carries a different density than the one specified. An unrealistic boundary layer results and the interior solution is greatly in error. Instead only the density of the inflowing water is specified. The horizontal gradient of density is set to zero in outflowing regions. The predictive equations for salinity and temperature states that the time change of density is due to advection and turbulent diffusion. Dilution by fresh water maintains the horizontal salinity gradients. The fresh water source is at the surface and so tends to stably stratify the estuary. There are no fluxes of salt or heat through the surface or bottom.

Equation of state

The equation of state for sea water expresses the relation between density and temperature, salinity and pressure. In a shallow estuary pressure effects can be ignored and the density can be represented as, $\rho = \rho_o ( 1 + \sigma_t 10^{-3} )$

where $\sigma_t$ is defined from Knudsen's Hydrographical Tables, (1901).

Dynamical balance

A Boussinesq dynamical balance is considered along the vertical-longitudinal plane of the channel. The density variations do not affect the accelerations or frictional terms. The cross channel balance can be approximated by geostrophy (Pritchard, 1956, Stewart, 1957), in which the pressure gradient adjusts itself to variations in the long channel flow. The vertical accelerations are negligible and the pressure gradient adjusts itself to variations in the density field. The longitudinal momentum equation can be written as,

$$\frac{\delta u}{\delta t} + u\frac{\delta u}{\delta x} + w\frac{\delta u}{\delta z} = -\frac{\delta \Pi}{\delta x} + \frac{\delta}{\delta x}\left(A_h \frac{\delta u}{\delta x}\right) + \frac{\delta}{\delta z}\left(A_v \frac{\delta u}{\delta z}\right) \qquad 2$$

where $\Pi$ is the pertubation pressure which remains after the hydrostatic pressure due to water of a constant density, $\rho_o$, is substracted and $A_h$, $A_v$ are the horizontal and vertical eddy viscosities. The coriolis acceleration, -fv, as well as the lateral advection of lateral shear, $v\frac{\delta u}{\delta y}$ are eliminated by making the canal assumption. The cross channel velocity, v, and its derivative, $\frac{\delta v}{\delta y}$ is negligible at the center of the channel. It is present at the sides in order to allow for acceleration and deceleration of the flow due to width variations. It does not contribute to the long channel dynamics, however.

In the vertical direction the gravitational acceleration predominates. The pertuabation pressure gradient adjusts to variations in the vertical density gradients. The equation can be written,

$$0 = -\frac{\delta \Pi}{\delta z} + \rho g \qquad 3$$

where $\rho$ is the variation of density from a mean value $\rho_o$ and $\Pi$ is the variation from the hydrostatic pressure due to that mean density.

A vorticity equation (Fig C ) for the component of vorticity perpendicular to the vertical plane x-z, is obtained by cross differntiations of ( 2 ) and ( 3 ).
The voritcity is defined as the vertical shear of the horizontal

velocity,

$$\eta = -\frac{\delta u}{\delta z} \qquad 4$$

The contribution due to the horizontal shear of the vertical velocity, $\frac{\delta w}{\delta x}$ is eliminated by the hydrostatic approximation.

The surface and bottom boundary conditions on the vorticity equation can be expressed as the stress . At the surface, the vorticity is proportional to the wind stress $\tau_w$.

At the bottom, it is proportional to the bottom stress $\tau_b$.

The stresses are obtained from a non-linear drag law,

$$\tau = C_D \rho u|u| \qquad 5$$

where $C_D$ is the drag coefficient which is about $2 \cdot 10^{-3}$. In the case of the wind stress, u is the wind velocity at ten meters height and $\rho$ is the density of air. The bottom stress is found using the water velocity and the mean water density $\rho_o$.

The boundary conditions for the vorticity equation on the open boudaries are that the vorticity be continuos,

$$\frac{\delta \eta}{\delta x} = 0. \qquad 6$$

This implies, through continuity, that the vertical shear of the vertical velocity is a constant on that boundary. The contribution to the vertical velocity of the density field is zero. The vertical velocity is linear with depth and is due to depth variations affecting the barotropic flow alone. In other words, the open boundary is in a region where the density flow is essentially horizontal.

The vorticity is predicted by the vorticity equations and appropriate boundary conditions. The vorticity is added to the estuary through wind stress at the surface and frictional stress at the bottom. Vorticity is generated internally by horizontal density gradients. Vorticity is advected by the flow and diffused by turbulent viscosities.

Continuity Equation

The approximation of incompressibility implies that the flow is

non-divergent. When the continuity equation in three dimensions is integrated across the channel (Pritchard, 1958) and the kinematic boundary conditions are applied, the following equation results,

$$\frac{\delta}{\delta x}(bu) + \frac{\delta}{\delta z}(bw) = 0 \qquad 7$$

The continuity equation( 7 ) is identically satisfied if we define a transport stream function, $\Psi$ ,

$$bu = -\frac{\delta \Psi}{\delta z} \qquad 8$$

$$bw = +\frac{\delta \Psi}{\delta x}$$

The vorticity is given by the equation,

$$\eta = \frac{\delta}{\delta z}\left(\frac{1}{b}\frac{\delta \Psi}{\delta z}\right) \qquad 9$$

The stream function is found by vertical integration of equation g and by application of the boundary conditions on the flow. The stream function is given on the bottom and at the surface,

$\Psi = \Psi(x)$ $\quad z = h(x)$

$\Psi = \Psi(x,t)$ $\quad z = 0$

The stream-function, $\Psi_B$, is zero on the bottom. The stream-function at the surface is due to the runoff transport and meteorological time dependent transports. The difference between the streamfunction at the surface and at the bottom in any vertical column is the barotropic transport (specified) through that section. The flow is obtained when equation g is integrated. The flow depends on the density structure through the vorticity generation term in the equation in fig c.

Turbulent processes:

The eddy viscosity coefficients (momentum diffusion) have been assumed to be independent of depth

$A_V = 40\ cm^2/s$ $\qquad A_H = 10^6\ cm^2/s$

The vertical eddy diffusivities (salt and heat diffusion) have been considered as a function of the stability

$$N^2 = \frac{g}{\rho}\frac{\delta\rho}{\delta z}$$

and the local shear

$$\eta = -\frac{\delta u}{\delta z}$$

$$K_V \sim \frac{\eta^2}{N^2}$$

The relation between the ratio $\frac{K_V}{A_V}$ and the density gradient and shear has been investigated by Kullenberg (1976) in the Baltic. The result can be summarized by the following,

$$\frac{K_V}{A_V} = \frac{R_{fc}}{R_i} \quad \text{for } R_i \quad R_{fc}$$

$$\frac{K_V}{A_V} = 1 \quad \text{for } R_i \quad R_{fc}$$

where $A_V$ has a minimum value (=40 $cm^2/s$).

$R_i = \frac{N^2}{\eta^2}$ $\quad R_{fc}$ = Critical Richardson flux number =0.1

If the wind speed exceeds 10 m/s $A_V = 40 \cdot \frac{\tau_W}{\tau_{W=10\ m/s}}$

This is meant to represent the extra turbulence created in Öresund by wind action. The wind is only allowed to increase the mixing above the main pycnocline.

Scales

The governing equations can be written in non-dimensional form by expressing all variables as the product of a characteristic scale and a non-dimensional variable. The resulting non-dimensional parameters determine the unique solutions to the equations. These parameters express the relative importance of processes.

The scales established in the model are as follows:

U -horizontal velocity scale = 1 cm/sec

L -horizontal length scale = $10^5$ cm

Z -vertical length scale = $10^2$ cm

| | |
|---|---|
| g | -gravity = $10^3$ cm/sec$^2$ |
| $\sigma$ | -scale of $\sigma_T$ = $10^{-3}$ |
| S | -salinity scale = 1‰ |
| T | -temperature scale = 1°C |

All other scales can be derived from these basic scales. The time scale, for example, is L/U = $10^5$ sec.

No vertical salt flux : $wS = K_v \frac{\partial S}{\partial z}$

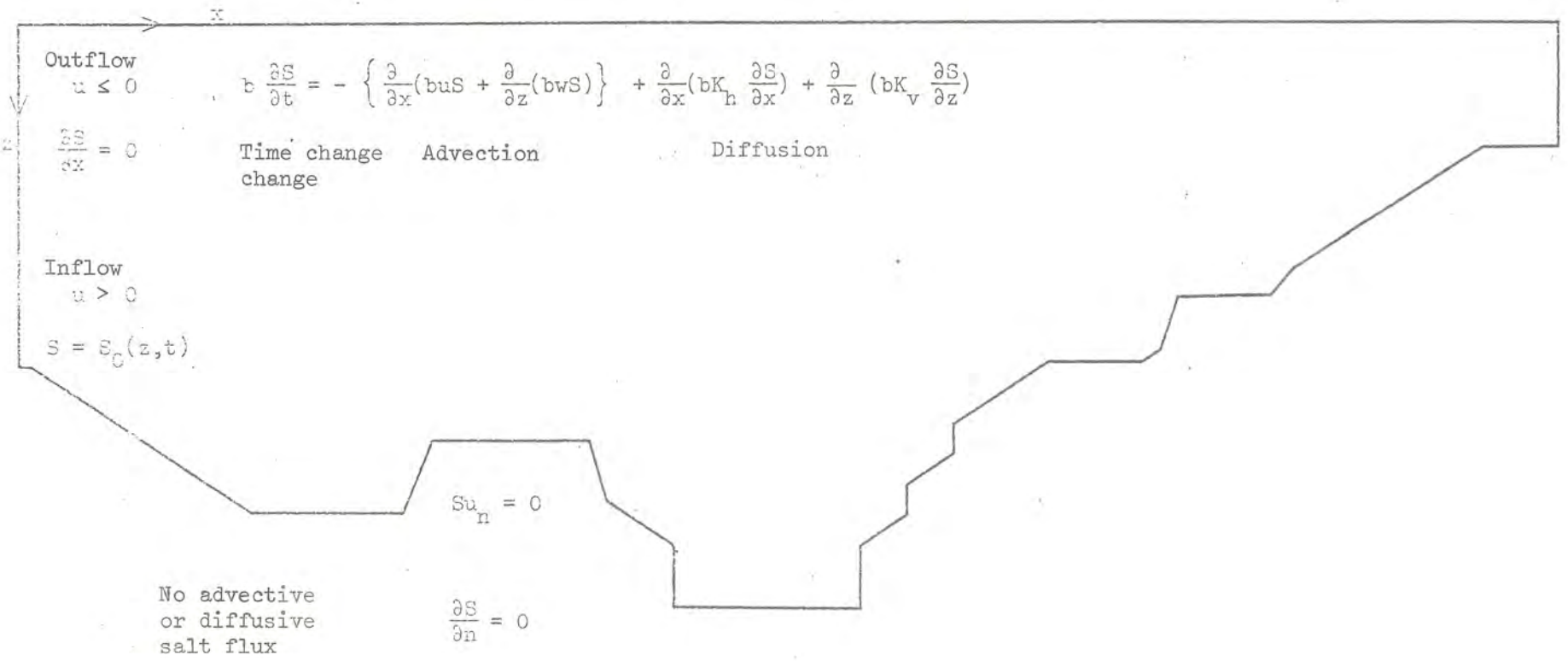


The salt equation and boundary conditions. Figure 3

Net vertical heat flux: $wT = K_v \frac{\partial T}{\partial z}$

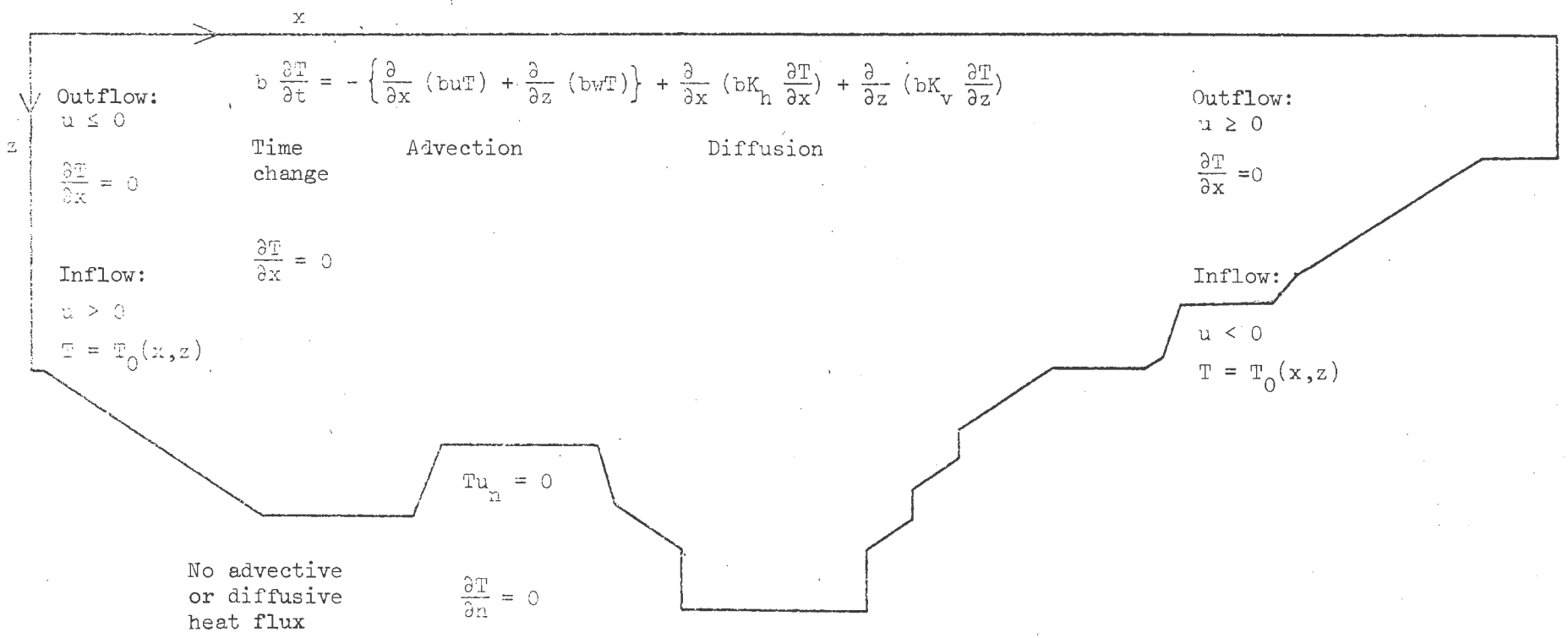


The heat equation and boundary conditions. Figure 4

$$\eta = \frac{\tau_{wind}}{A_v \rho_0}$$

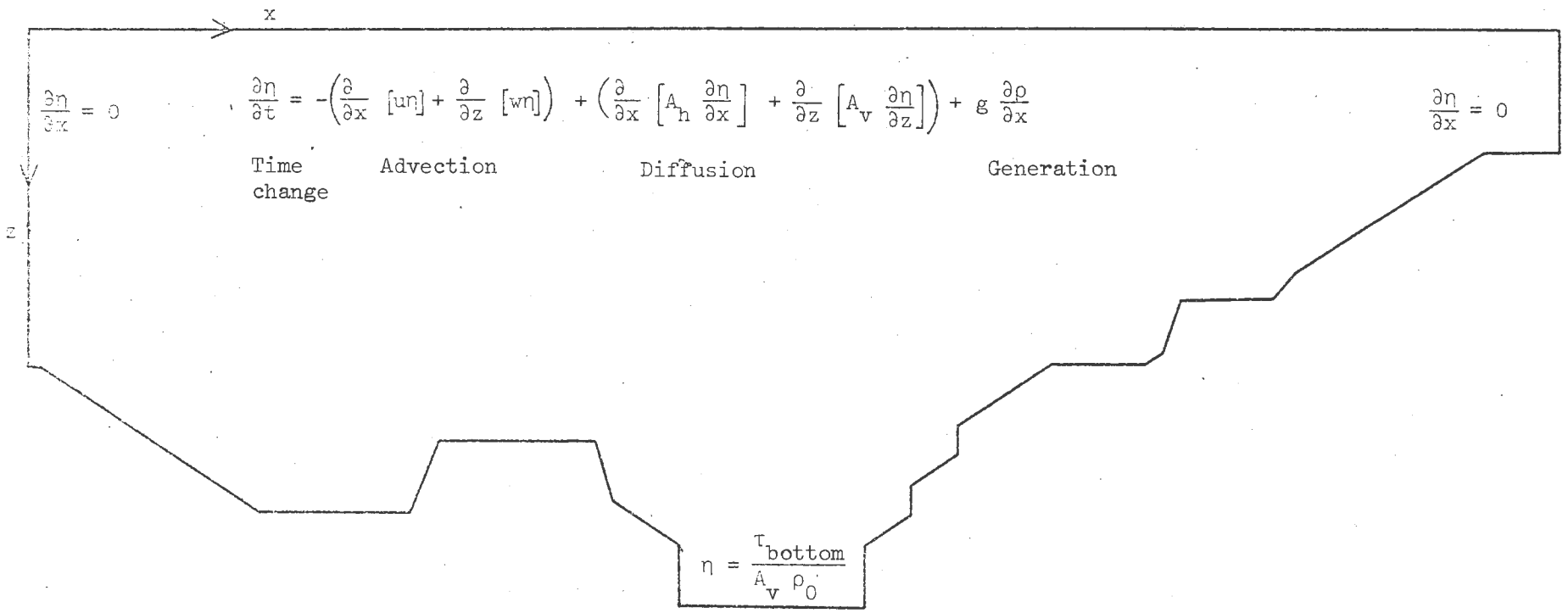


The vorticity equation and boundary conditions. Figure 5

$$\Psi_{surface} = \Psi_{runoff} + \Psi_{meteorological}$$

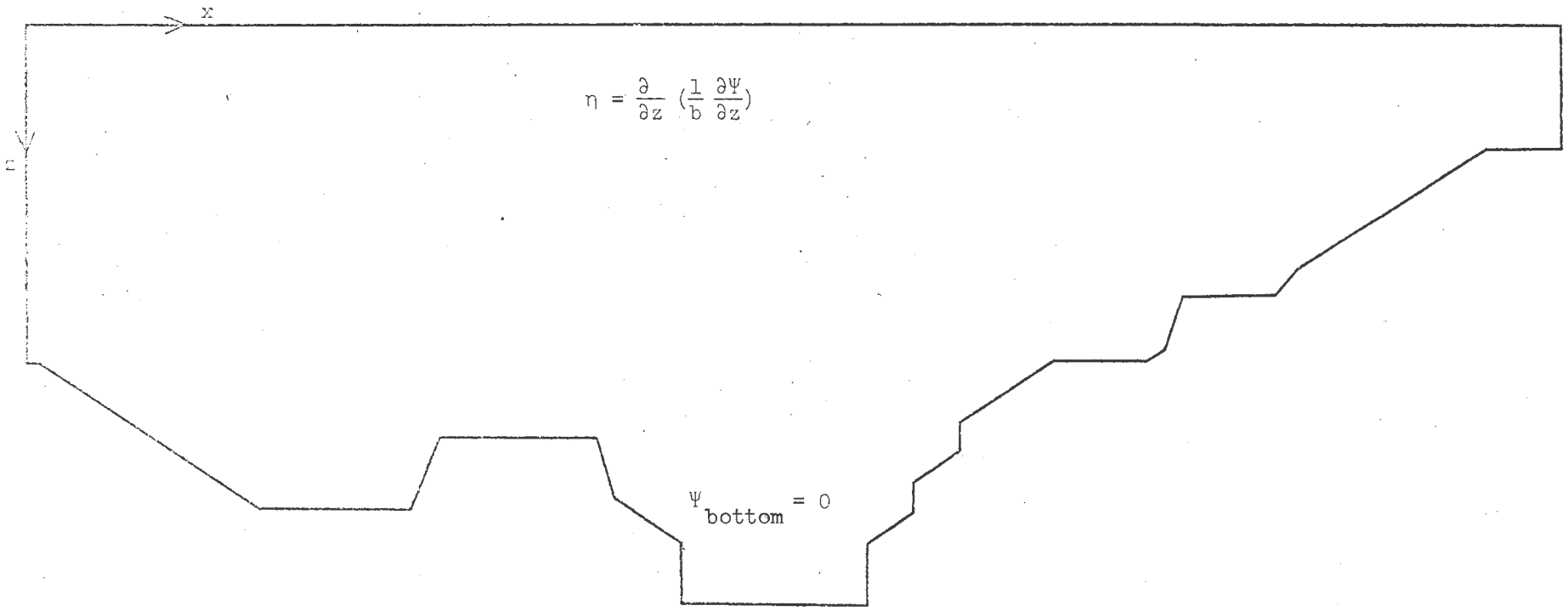


The streamfunction equation and boundary conditions. Figure 6

## 4. NUMERICAL METHOD

### 4.1 NOTATION

The non-dimensional equations and their boundary conditions are a predictive set and can be numerically integrated in time from a known initial field. The variables are defined on a grid (Fig E). Finite difference approximations to the equations are written. The sum and difference operators adopted by Shuman (1962) are used throughout:

$$\overline{(\quad)}^{x} = ((\quad)_{i+1/2} + (\quad)_{i-1/2})/2$$

$$(\quad)_x = ((\quad)_{i+1/2} - (\quad)_{i-1/2})/\Delta x$$

### 4.2 NUMERICAL FORMULATION

The leapfrog scheme is used for the time differencing. The prediction at the n+1 time level is determined from evaluation of the variable at the n-1 level, the advection and sources and sinks at the n time level and the diffusion in the horizontal as a "lag", that is, at the n-1 level. The vertical diffusion is implicitly represented as the average of the n+1 and n-1 time levels. The implicit scheme is used for vertical mixing so that the small grid spacing in the vertical direction does not unnecessarily restrict the time step. Each vertical column is represented as a tri-diagonal matrix equation which is solved using a variation of the Gaussian elimination. The advection terms have been represented in Arakawa (1966) form to eliminate non-linear instability.

The equation of state is computed in the form suggested by Friedrichs and Levitus (1972). It requires less computer time than the Knudsen (1901) form.

### 4.3 NUMERICAL PROCEDURE

The procedure to obtain the solution as a function of time can be summarized as follows:

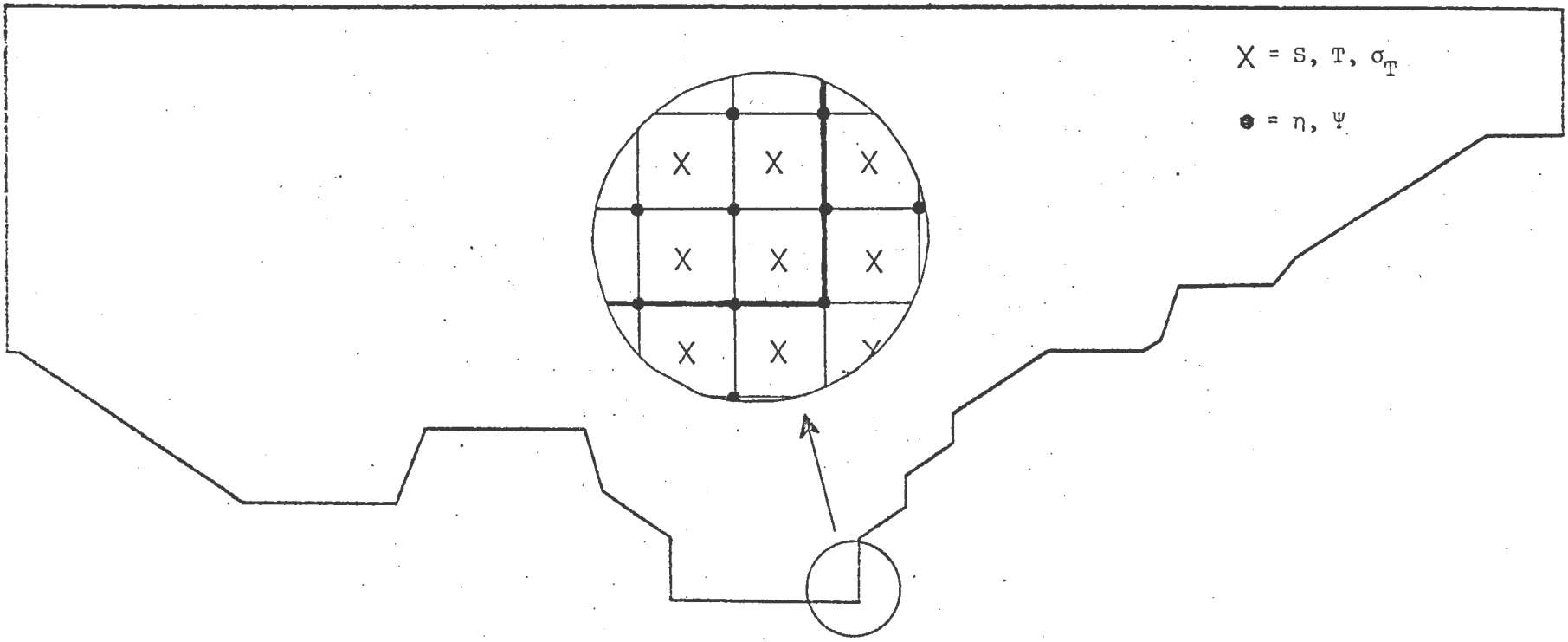


The finite difference grid. Figure 7

1) initialization of the physical fields and parameters
2) time stepping of the salinity and temperature equations (Figs F and G)
3) computation of $\sigma_T$ (Fig I)
4) time stepping of the vorticity equation.(Fig H)
5) computation of the streamfunction (Fig J)
6) periodic suppression of the computational mode
7) output of the vertical mixing, temperature, salinity and streamfunction
8) return to 2) until computation with the physical fields is complete

No vertical salt flux: $(wS^{-z})^n = \varepsilon\left(\frac{S_z^{n-1} + S_z^{n+1}}{2}\right)$

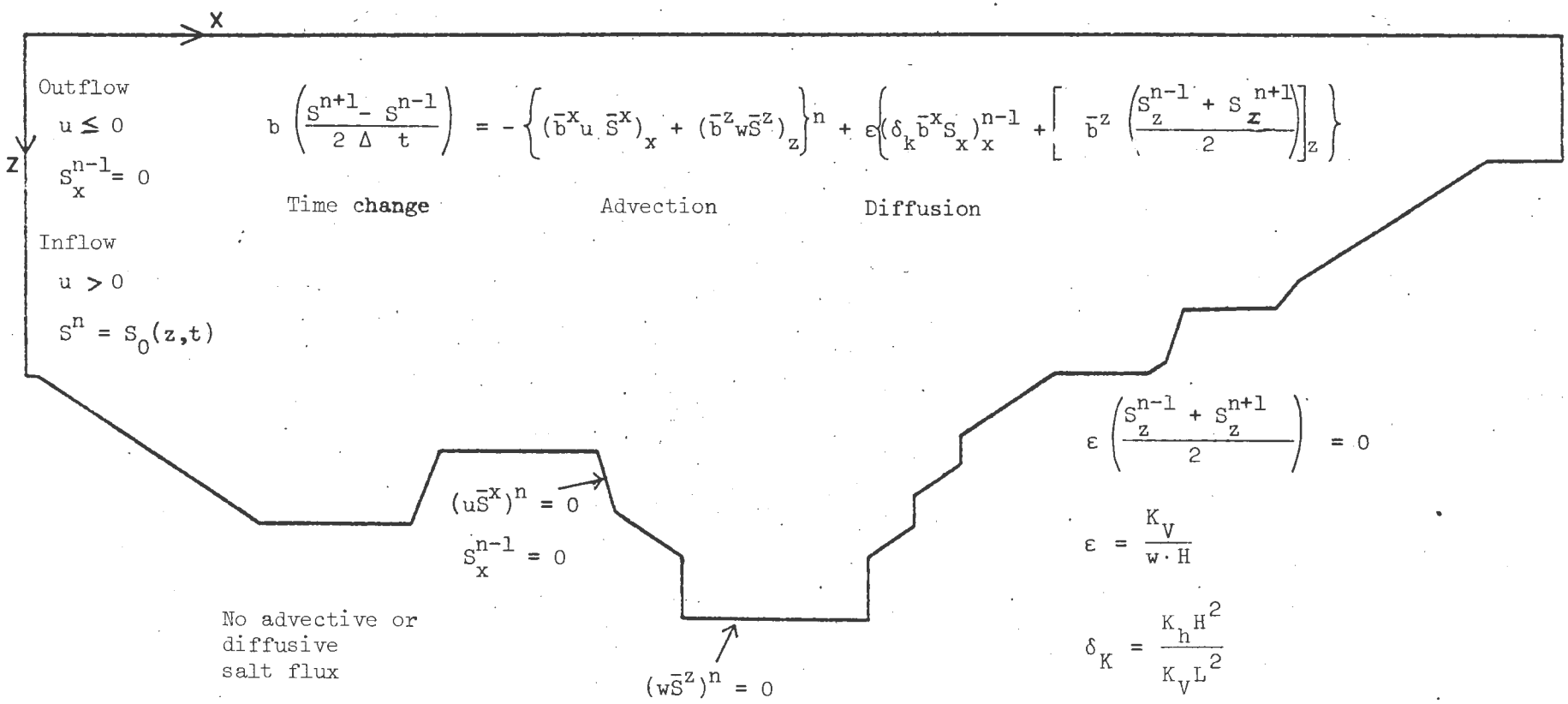


The finite difference salt equation and boundary conditions.

Figure 8

Net vertical heat flux: $(w\bar{T}^z)^n = \varepsilon \left( \frac{T_z^{n-1} + T_z^{n+1}}{2} \right)$

$$b\left(\frac{T^{n+1} - T^{n-1}}{2\,\Delta t}\right) = -\left\{ (\bar{b}^x u \bar{T}^x)_x + (\bar{b}^z w \bar{T}^z)_z \right\}^n + \varepsilon \left\{ (\delta_k \bar{b}^x T_x)_x^{n-1} + \left[ \bar{b}^z \left( \frac{T_z^{n-1} + T_z^{n+1}}{2} \right) \right]_z \right\}$$

Timechange — Advection — Diffusion

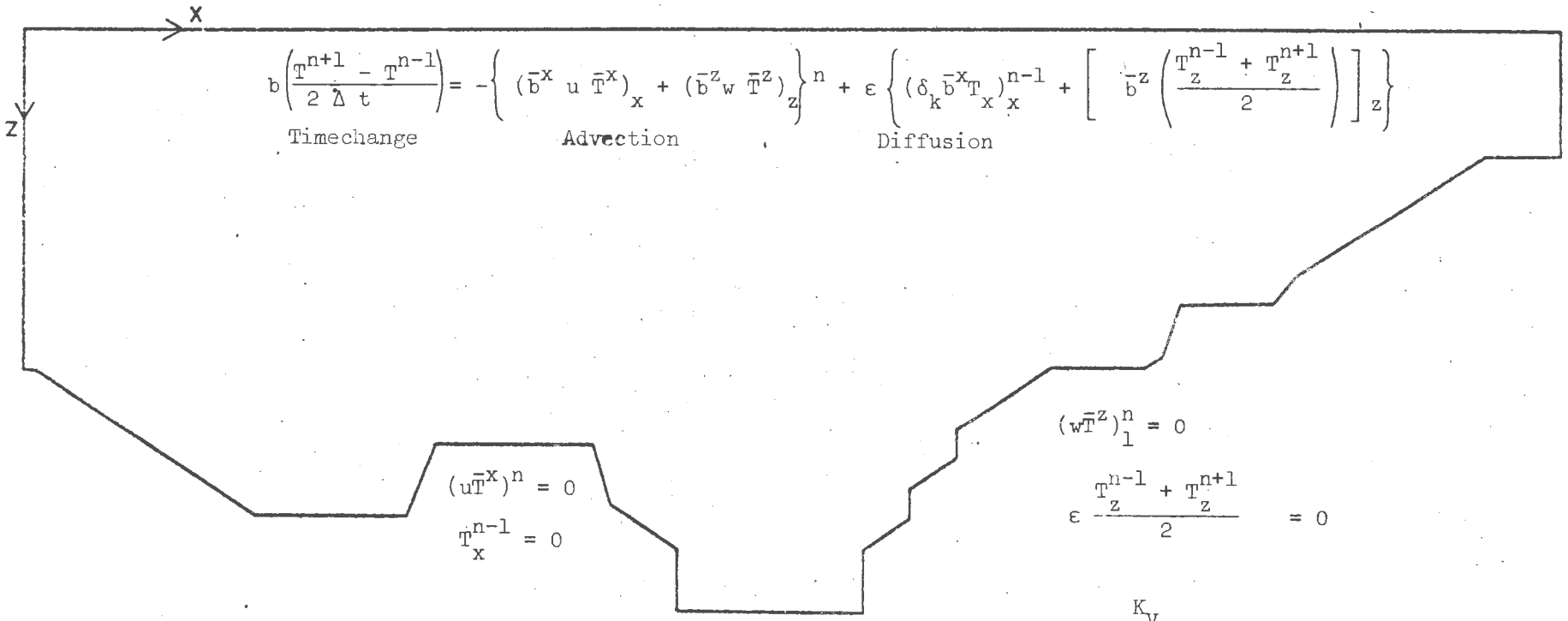


$$\varepsilon = \frac{K_V}{w \cdot H}$$

Outflow u 0

$T_x^{m-1} = 0$

Inflow u 0

$T_x^n = T_0(z,t)$

The finite difference heat equation and boundary conditions.

Figure 9

$$\delta_K = \frac{K_h}{K_V} \frac{H^2}{L^2}$$

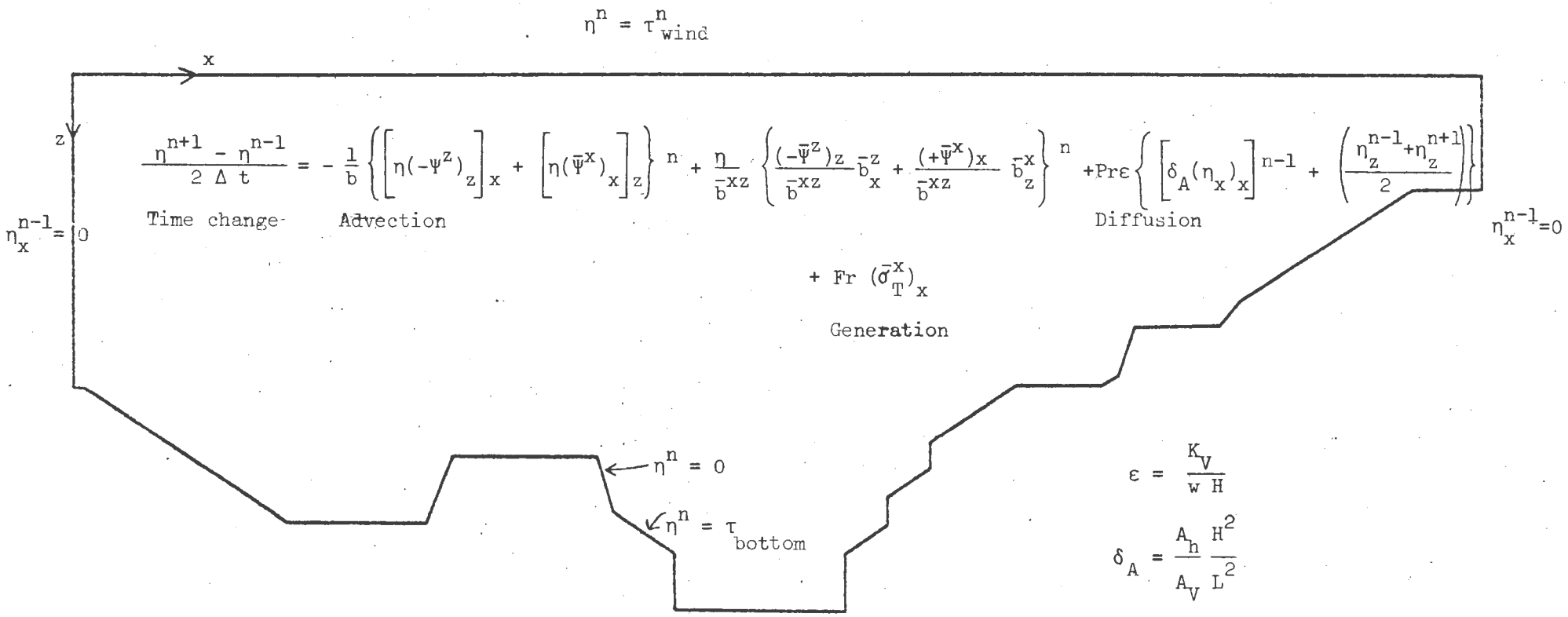


The finite difference vorticity equation and boundary conditions.

Figure 10

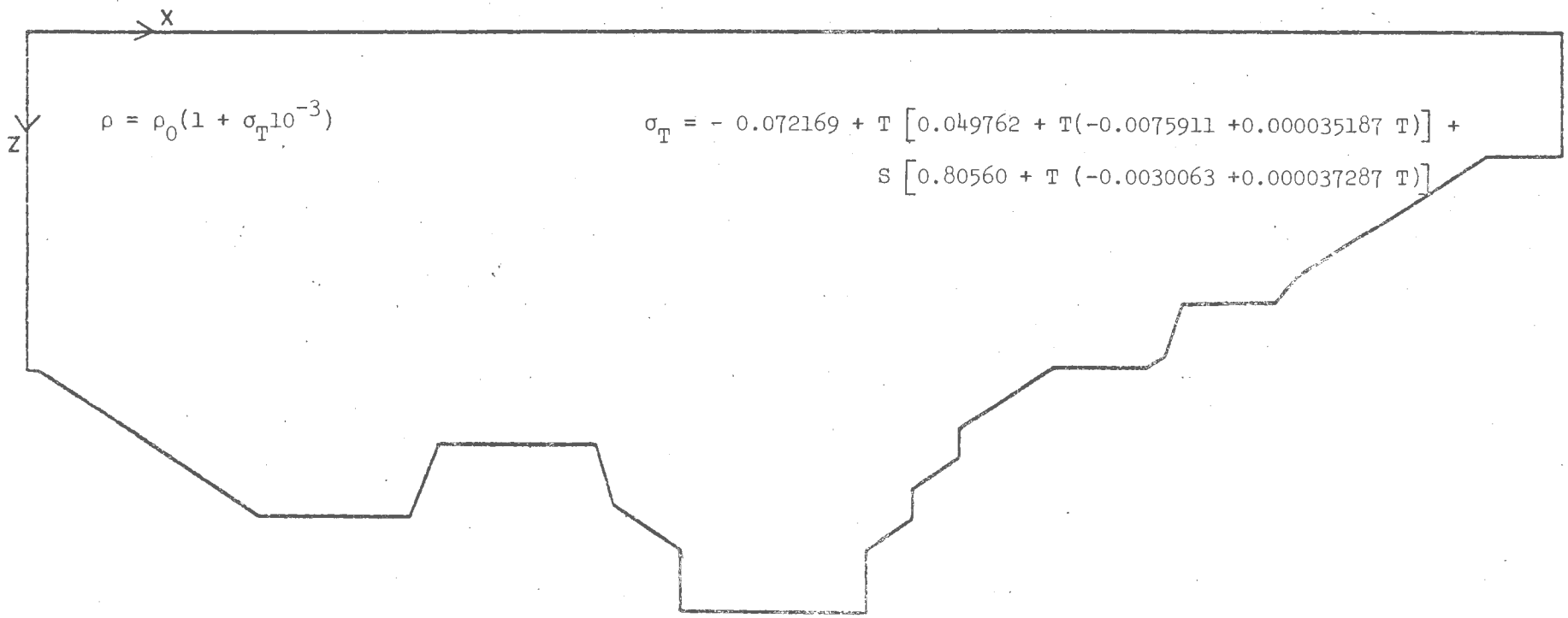


The finite difference equation of state. Figure 11

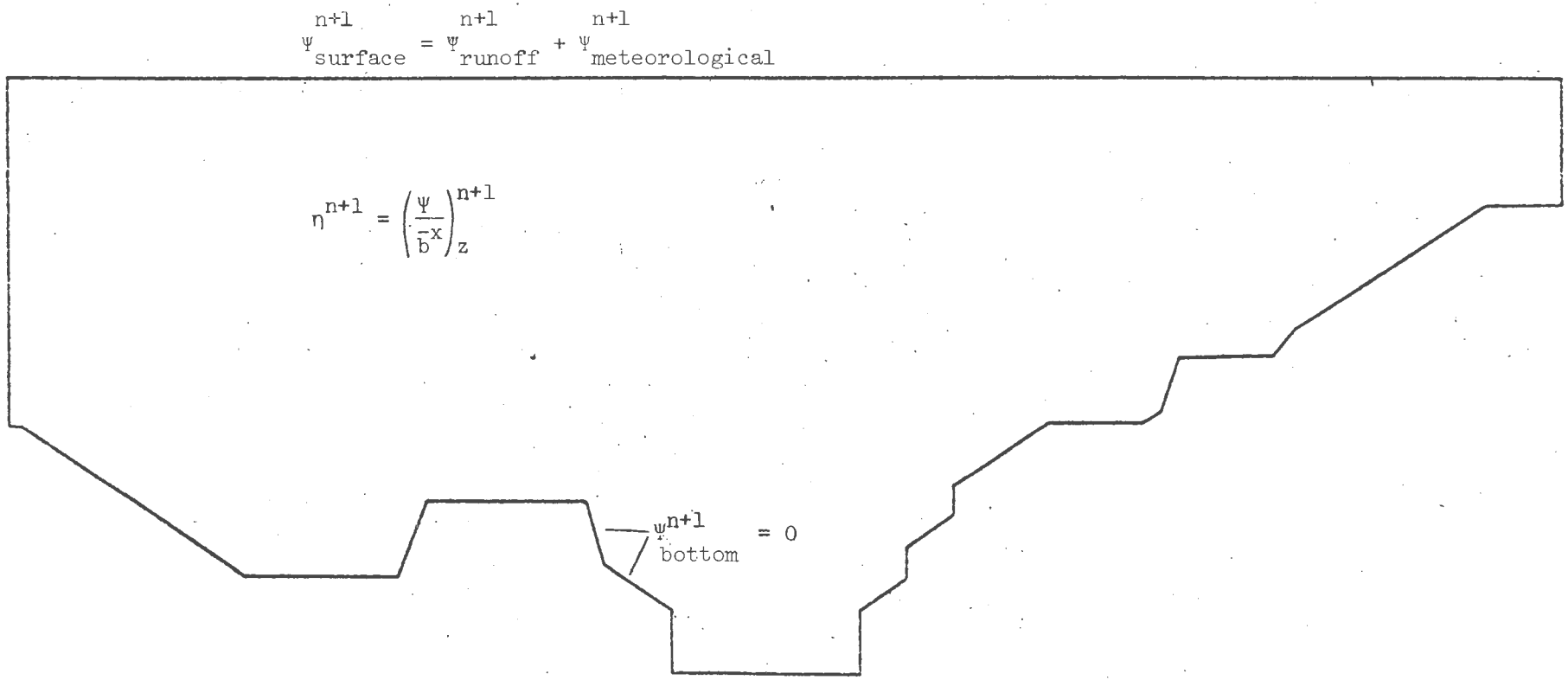


The finite difference streamfunction equation and boundary conditions.

Figure 12

FIELD MEASUREMENTS

In order to obtain data to verify the numerical models used for prediction of the effects of the tunnel, field measurements were carried out from April 27th to June 10th 1976. The program included recording instruments and observations from ships traversing Öresund. The number of waterlevel recordings in the Sound were increased during the period.

In the "Appendix" is shown which field measurements were carried out. The stations occupied by ships or recording instruments are shown in fig 13.

Recording instruments

The recording instruments were suspended from subsurface bouys. These were kept in position by three anchors. The periods in which the different meters were working properly is shown in fig 14a, b, c. The material has been separated into three groups: Correct record, Partly usable, Not usable. The lable "Correct record" has been given to periods during which the instruments recorded without errors and the bouy-system was in order. Partly uasble records are, for example where the depth of the subsurface bouy changed due to strong currents; and record containing only few erroneous recording. Periods when the bouy was at the surface or when seaweed prevented the revolution of the rotor for example are lebelled: Not usable. The instruments below the pycnocline were, during the last part of the study, especially exposed to floating weed.

Complementary measurements with recording temperature - salitnity - chains were carried out by Danish Hydraulic Institute. The location of these instruments is shown in fig 13. The instruments at Station 1 was damaged when recovered and the record was not usable. The other two instruments, however, recorded correctly.

Observations

During May samples were taken at Station 1, 1 a and 1 b. The sampling depth were however uncertain and the result was labelled: Not usable.

In eraly June 1976 a survey was carried out with two boats. The stations occupied are shown in fig 13. Each station was visited two times a day or more.

Water level recording

The location of the Swedish instruments are shown in fig 13. The recording at Klagshamn is of good quality while errors (in the paper feeding in the recording instrument) at Viken were found. The records from Landskrona and Falsterbo is of a low quality.

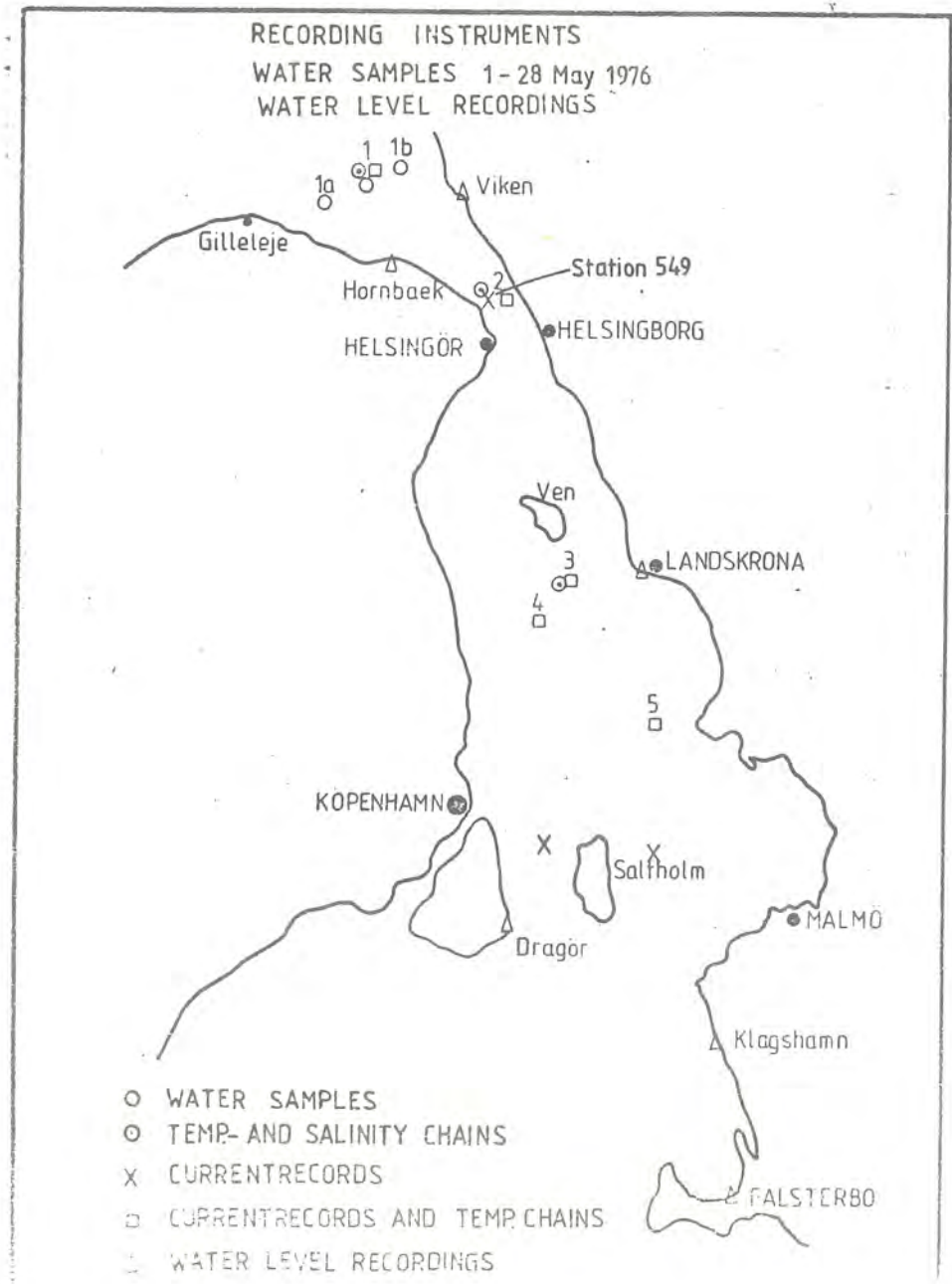
RECORDING INSTRUMENTS
WATER SAMPLES 1 - 28 May 1976
WATER LEVEL RECORDINGS
1
1b
1a
Viken
Gilleleje
Station 549
Hornbaek
2
HELSINGÖR
HELSINGBORG
Ven
3
LANDSKRONA
4
5
KÖPENHAMN
Saltholm
MALMÖ
Dragör
Klagshamn
FALSTERBO
WATER SAMPLES
TEMP.- AND SALINITY CHAINS
CURRENTRECORDS
CURRENTRECORDS AND TEMP. CHAINS
WATER LEVEL RECORDINGS

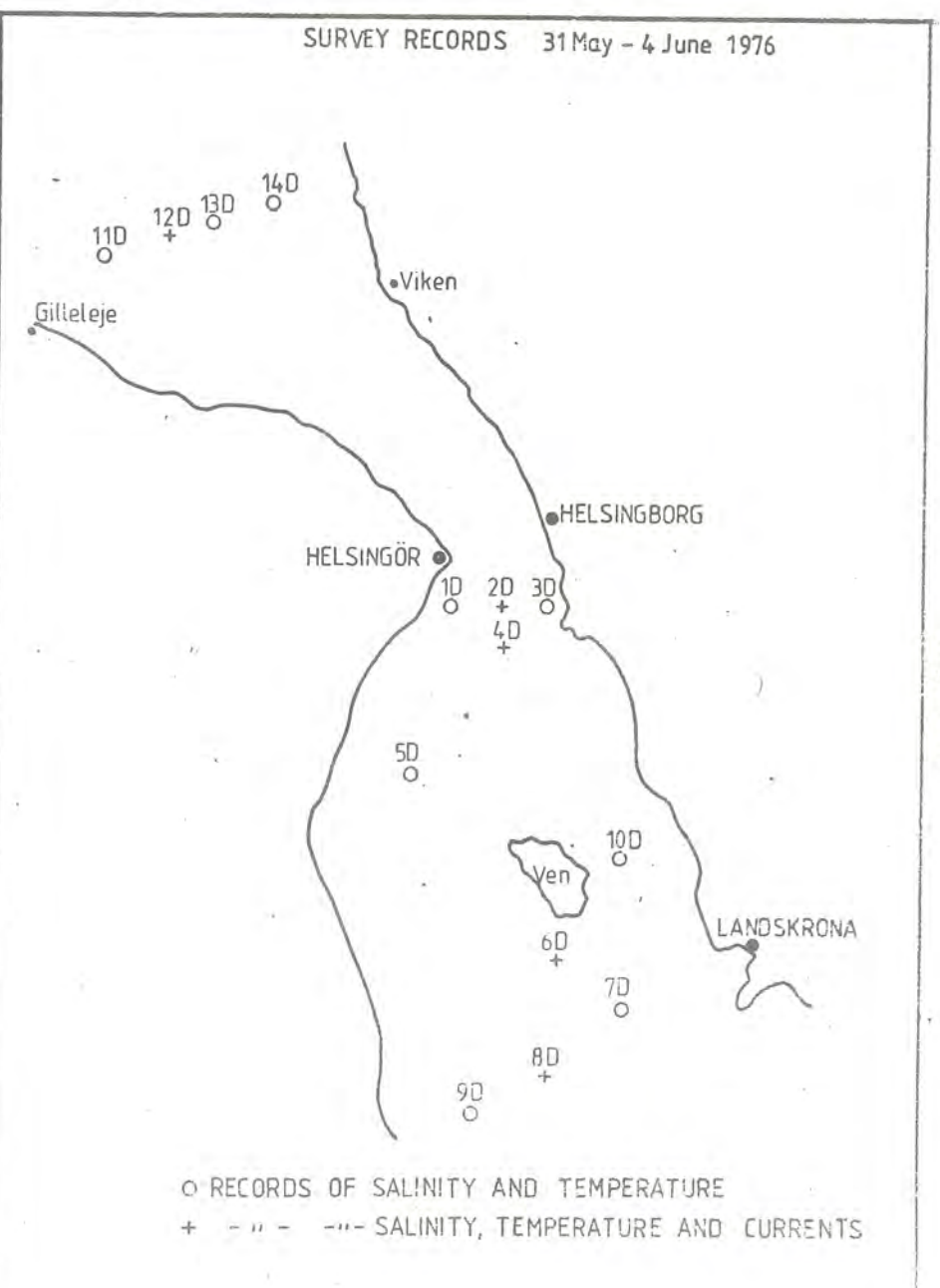
SURVEY RECORDS 31 May - 4 June 1976
11D
12D
13D
14D
Viken
Gilleleje
HELSINGBORG
HELSINGÖR
1D
2D
3D
4D
5D
10D
Ven
LANDSKRONA
6D
7D
8D
9D
RECORDS OF SALINITY AND TEMPERATURE
+ - " - -"- SALINITY, TEMPERATURE AND CURRENTS

Figure 13

## MODEL VERIFICATION

Two periods during the field measurements carried out in May-June were selected to test the model. During the first period, (May 12 - 15), most of the recording current meters were working correctly. This period is therefore suitable for verifying the currents. The second period, (May 29 - June 1) contained the most intense field measurements including both recording current meters, temperature and salinity records, as well as measurements taken from ships continously cruising in the Sound. Unfortunately the current meters in the lower layers did not work properly during this period, which implies that only indirect verification of the current in the lower layers can be made. However, the period is suitable for verifying the mixing.

The second period was actually studied first and it seems logical to discuss the result in the same order.

The salinity and temperature at the Baltic boundary were almost constant during both periods. (The bounday data, used when the transport was computed to be into the model, were taken from a recorder near the southern boundary). The boundary data were taken constant with depth. (The depth at the boundary being only 8 meters).

In the Kattegatt values from a thermistor chain were taken as boundary values for temperature. Profiling of salinity was carried out from ships and a T-S diagram with all salinity values from both verification periods was constructed. The T-S curve shows that the relationships between temperature and salinity did not change during the verification periods. Thus the boundary values for salinity were constructed from measured temperatures and the T-S relationship. New boundary values were given every hour.

Water level records from Hornbeck and Viken at the northern end of the Sound and from Klagshamn at the southern end were used in a one dimensional channel model to compute the

integrated transport due to water level differences between Kattegatt and the Baltic. The transport values computed were fed into the two-dimensional model as barotropic forcing.

It should again be mentioned that the model boundary conditions are such that at a level where the current is out of the model the boundary valuea are set equal to the value at the first interior point. In other words, the model is allowed to find its own boundary value. At a level where an inflow is computed, the model is using given boundary values, for example: measured temperatures or salinities.

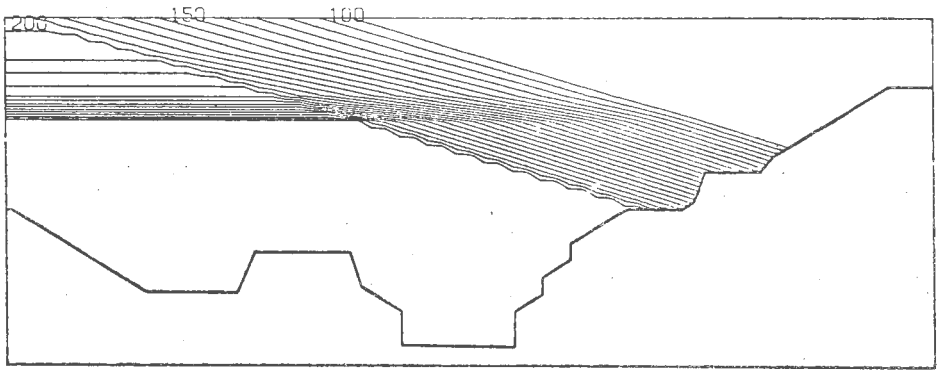


Figure 14. Initial salinity field.

The current and density fields used as initial conditions for the verification runs were totally artificial. Starting from zero velocity and with the salinity and temperature distribution shown in fig 14 the model was run for 6 days with constant boundary conditions. The constant boundary salinities and temperatures used were similar to the starting values for the verification period studied. The boundary transport was small. The salinity and current field after 6 days are shown in fig15.

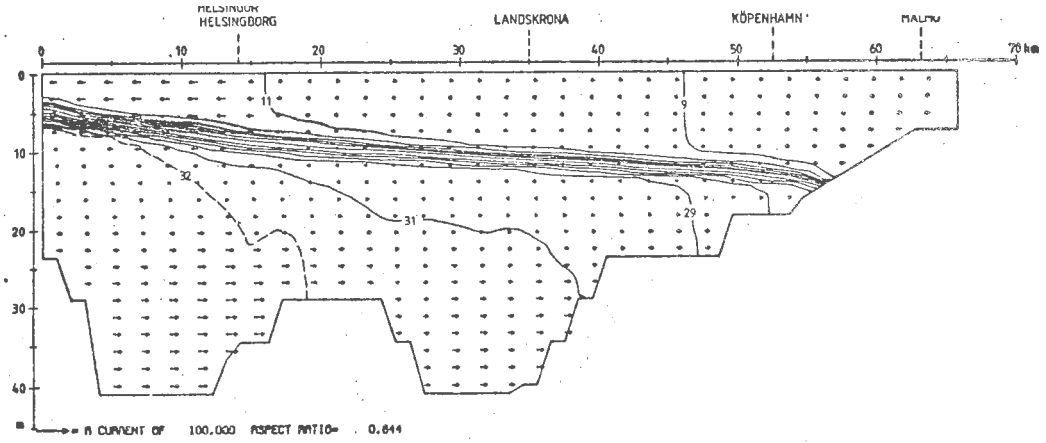


Figure 15.

Agreement between the model and reality is consequently not achieved by starting the model with measured internal salinity- and temperature fields. The model itself with the needed boundary conditions, its inbuilt mixing assumptions etc., is able to compute natural fields from artificial initial fields.

The wind stress and bottom friction were computed with the formula:

$$\tau = C_D \cdot \rho \cdot u \cdot |u|$$

where $C_D = 0.002$

$\rho$ = density of air or water

$u$ = wind at 10 m hight or current velocity at the gridpoint closest to bottom

The vertical eddy coefficient for momentum $A_V$ is a constant.
$A_V = 40\ cm^2/s$

The vertical eddy coefficient for salt and heat $K_V$ varies with the density stratification and the shear.
The horizontal mixing coefficients are constants.
$A_H = K_H = 10^6\ cm^2/s$.

Verification period 29 -31 May 1976

The prevailing winds were mostly weak to moderate. However, a west to northwest wind with a velocity of nearly 10 m/s was blowing on the 31st. This wind together with a weak low, piled up water in the southern Kattegatt and drove the water of Öresund south at all depths.

Currents

The computed currents were compared with recorded values at Stations 2, 3 and 5 and at Station 549 from the Danish Belt Project. (See fig 16). At 7 m depth the computed currents show the same behavior as the along channel component of the recorded current. Station 2 and 549 are difficult to compare to the computed current because of the big difference between the recordings of the stations. The agreement between computed currents and Station 2 is, however, good. The agreement at

the other two stations are also acceptable if one bears in mind theat the computed current is a mean over the width of the channel and that recordings were taken at the Swedish side.

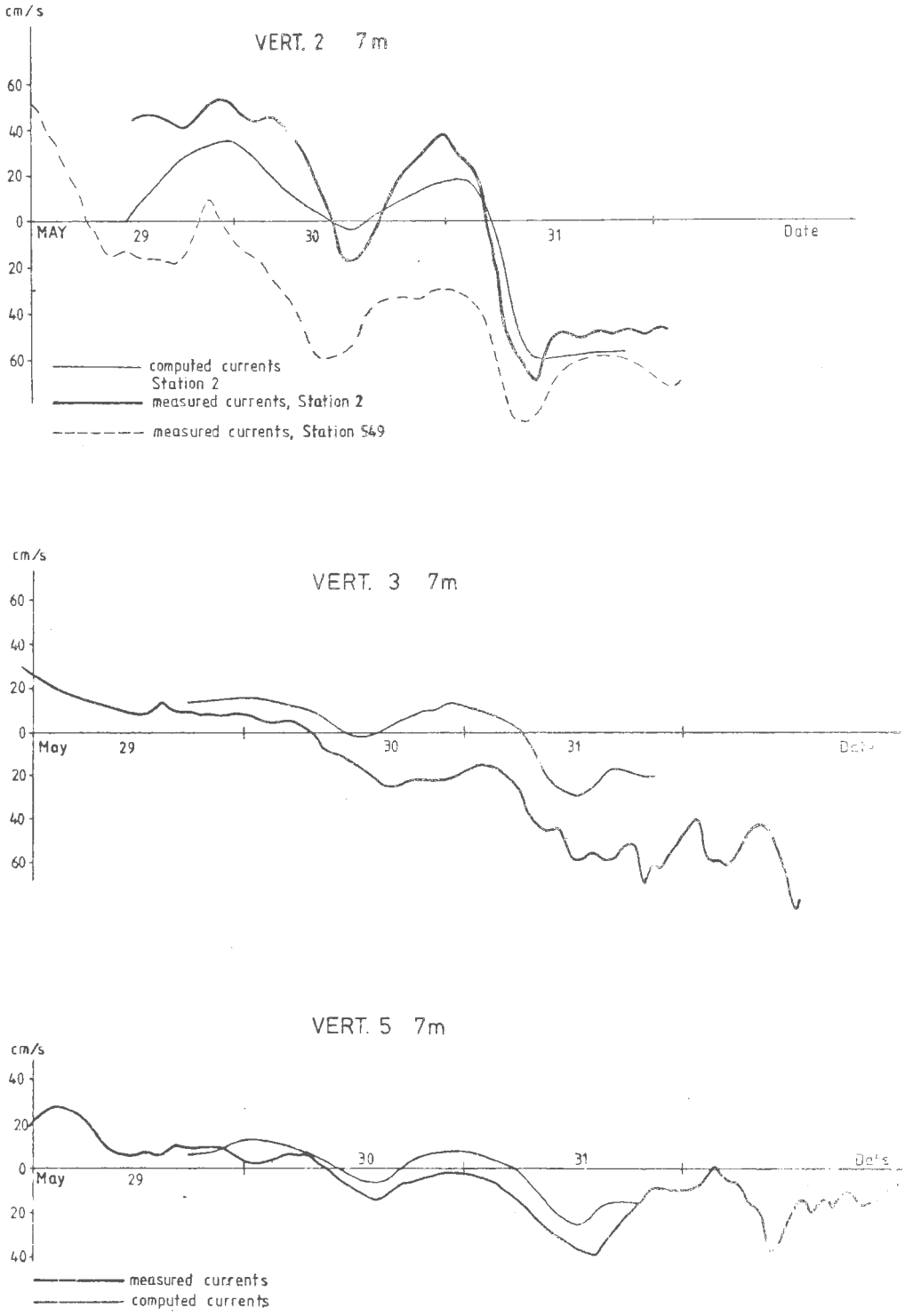


Figure 16. Computed and recorded currents.

The agreement at 14 m, Station 2, is poor. This can be due to the fact that the pycnocline and the turning point for the current is close to 14 m. A slight error in the real depth of the current meter and/or an error of the computed depth of the pycnocline results in large derivations of the current values. The poor agreement can of course also be the result of an error in the computed current profile.

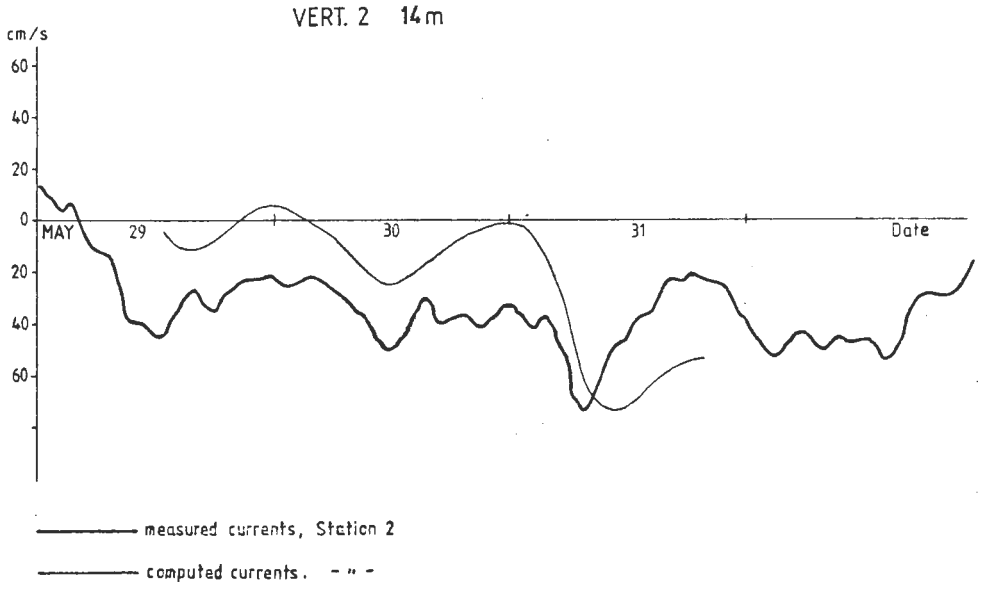


Figure 17. Computed and recorded currents.

Because of the lack of current records from deeper layers during the first verification period the verification of the deep current had to be done in an indirect way. The thermocline boundary between the salt water and the brackish water is very sharp and well recorded by a temperature conductivity chain and a thermistor chain at Station 3 and by hand-made measurements in a section across the Sound near Station 3. The recorded thermocline (as recorde from e.g. the TC chain) rises about two meters between 75-05-30 at midnight and 76-05-31 at 8 p.m. The intransport in the lower layer causes this change.

The computed transport in the lower layer results in a rise

of the thermocline to the same level as the measured one. This indicates that the computed transport in the lower layer is of the right magnitude (see fig 18).

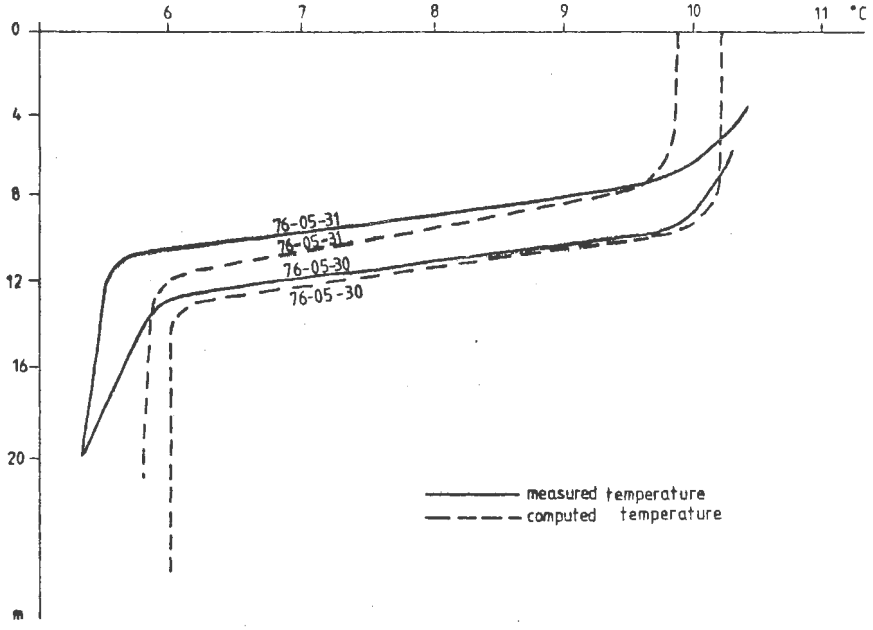


Figure 18. Temperature at Station 3, 30 of May at midnight and 31 of May at 8 P.M.

Mixing

The vertical mixing coefficient for salt and heat used varies with density stratification and velocity changes as explained above. For small density gradients and/or large shear stresses the value of $K_V$ ($K_V$ = turbulent diffusion coefficient for salt and heat) is the same as the turbulent diffusion coefficient for momentum $A_V$. Momentum mixing is not so strongly decreased by a density gradient as is the mixing of salt and heat. A water body transported from the salt water up to the brackish layer loses its momentum fast, but can return to the salt layer without being mixed altogether with the brackish water. The ratio between $K_V$ and $A_V$ is, thus, decreasing where there is increasing density gradient.

In the work by Kullenberg (1976), a form for the dependence of $K_V/A_V$ on the stratification and the shear is given. The formula is based on dye experiments in open waters and is regarded as more applicable in this study than results from

tank experiments. However the experiments only give a value of the ratio $K_V/A_V$. Although it is quite clear that there is a dependence of density stratification also on $A_V$, the value has been kept constant in this study due to lack of information on how $A_V$ should change.

As an example of the resulting mixing coefficient $K_V$ a situation from 31.5 is discussed. In figure 19 one can study the computed salinity gradient.

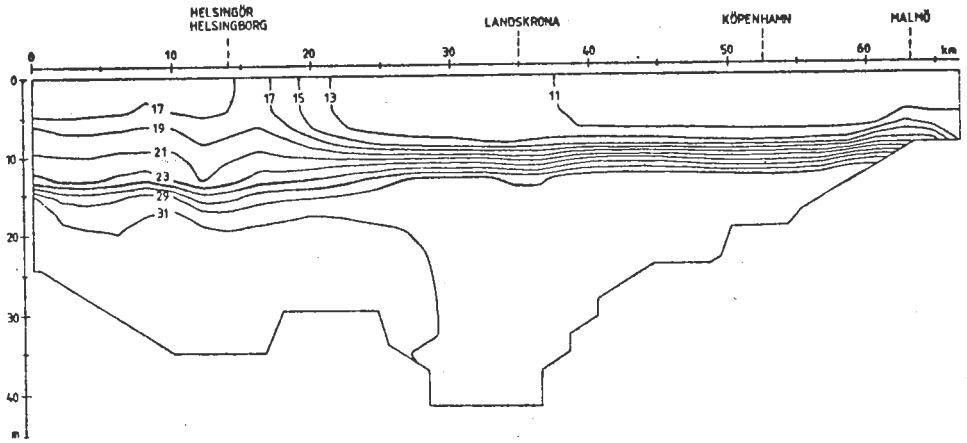


Figure 19.

In the northern part of Öresund a rather weak vertical gradient is advected into the Sound from Kattegatt accompanied by a steep horizontal gradient in the surface layer. In the southern part, the steep vertical gradient from the earlier existing current system is still persistent. Figure 20 shows the vertical mixing coefficient $K_V$. One plot is from the northern part of Öresund, the other from the south. The vertical current shear at the two locations is about the same.

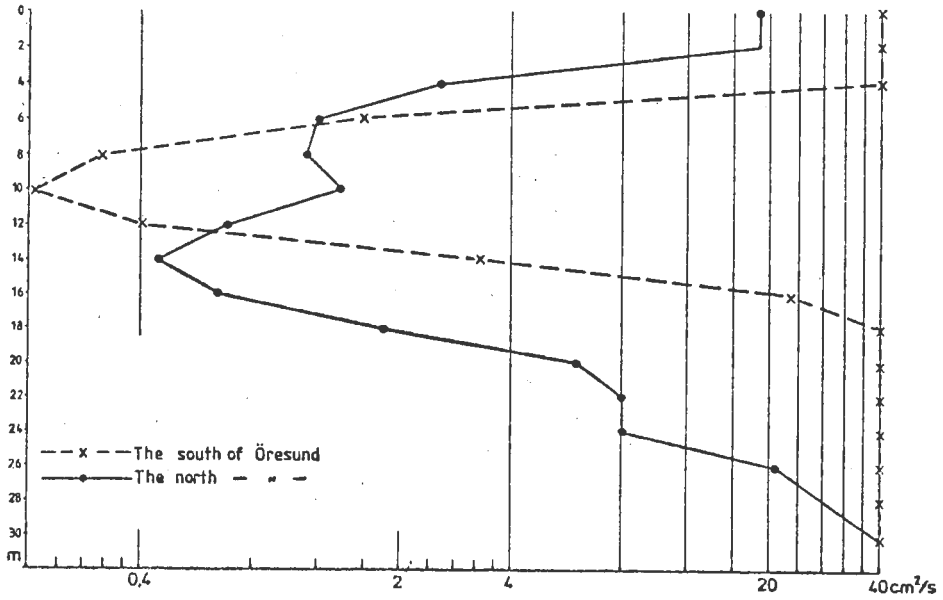


Figure 20. The eddy diffusion coefficient $K_V$.

The form of mixing introduced in the model can be verified by studying figure 18. The vertical temperature gradient computed compares well with the recorded stratification.

The vertical gradient in a model can be advected in from the boundary and therefore be purely defined by the boundary conditions. The situation in fig18, however, was created by a north-going current at the surface and a south-going current in the bottom waters which means that the gradient is created by mixing the surface water, whose salinity and temperature were defined by the boundary condition at the Baltic boundary, with the bottom water settled at the Kattegatt boundary. The surface temperature and the temperature in deep waters in fig 18 do not coincide exactly with the computed values. This depends on small errors in the boundary data. However the computed depth of the thermocline is correct and the sharpness of the gradient is also very well reproduced in the model.

Verfication period 12 -15 May 1976

The second verification was carried out with the same mixing and friction coefficients and the same boundary structure as the first one. The initial fields were again created from artificial ones.

The winds during the period were strong most of the time. Before the verification period started, a strong south-east wind had prevailed for about two days. After a few hours of north wind during the 12th, another storm from the south carried surface water from Öresund out into Kattegatt. On the 14th the wind turned west and north-west and the weather situation and water level changes forced the water south through Öresund at all depths.

Currents

The computed currents were compared with recorded values at Stations 2 and 5 and at Station 549 from the Danish Belt project. Between Helsingborg and Helsingör there were two strings of current meters (Stations 2 and 549). One string with meters at 7 and 25 m depth was in the center of Öresund. Another with meters at 7, 14 and 19 m depth was closer to the Swedish coast (fig 13).

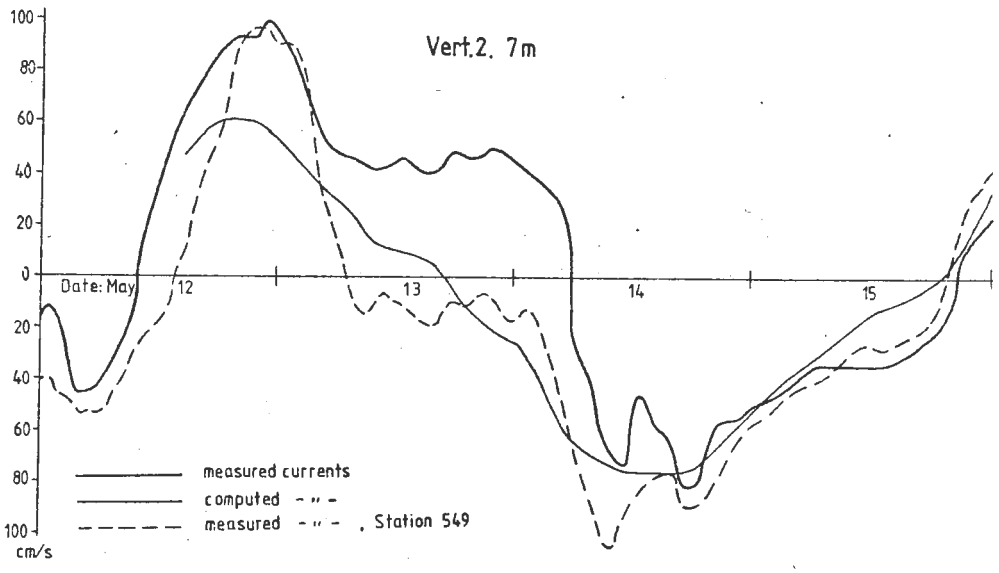


Figure 21 a.

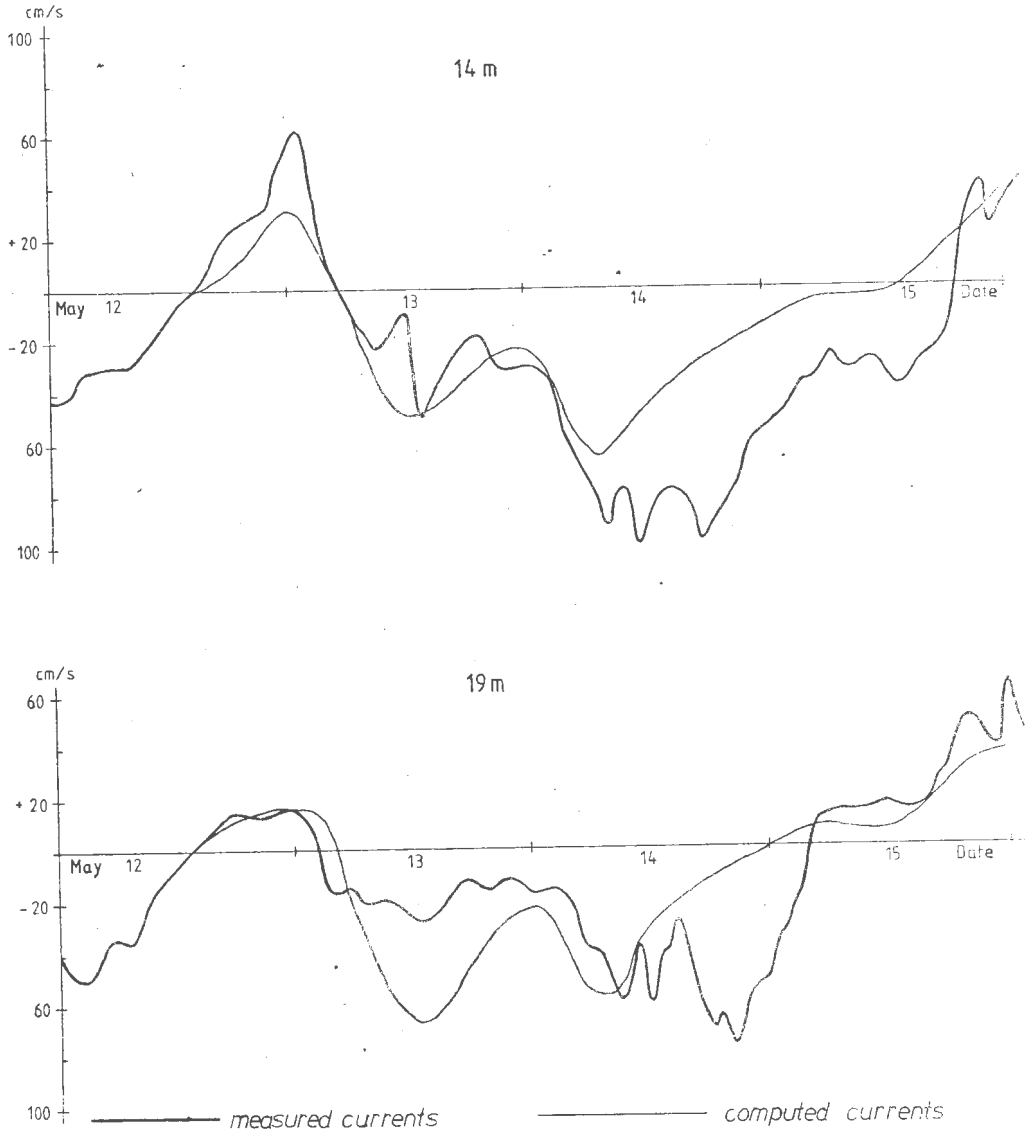


Figure 21 b.

Comparison between the along channel component of the measured currents and the computed currents shows that there is good agreement at 7 m depth between the computed values and the recorded values from the center of the channel.

During the first half of the verification period there is a rather big difference between the different recording stations. The outgoing current at the surface is stronger at the Swedish coast probably due to the rotation of the earth (Coriolis effect). During the last half of the period, the computed current agrees very well with the recorded one

at both stations. At 14 and 19 meters depth (see fig 12 b) the agreement is also good exept for some hours at the 14th. There is then a marked peak in the velocities which is totally absent in the model results. The reason is the following: On the morning of the 14th there was a south-going current running at all depths. The salinity recordings imply that there was a two layer system with a horizontal boundary between the layers. At midday when the wind turned from south to west (wind velocity 12-15 m/s) it forced the surface layer towards the Swedish coast. For a few hours all meters at the Swedish side were recording in the surface layer. This theory is supported by the salinity records, especially the record from 19 m which shows a marked decrease in salinity during the episode from normal deep water salinity (28-30 ‰) to a salinity value normally found in a south-going surface layer (20-21 ‰, see fig 22).

When the strong current at 19 m ceased the salinity went back to the high value indicating that the pycnocline again was close to horizontal. The wind was by then north-west and the wind speed was decreasing. The model computes the current averaged over the width at every depth and can not represent a situation where there is a big difference between the two sides of Öresund. The computed mean current is, however, representative of the transport as the slope of the pycnocline does not affect the volume transported in an axisymmetrical channel.

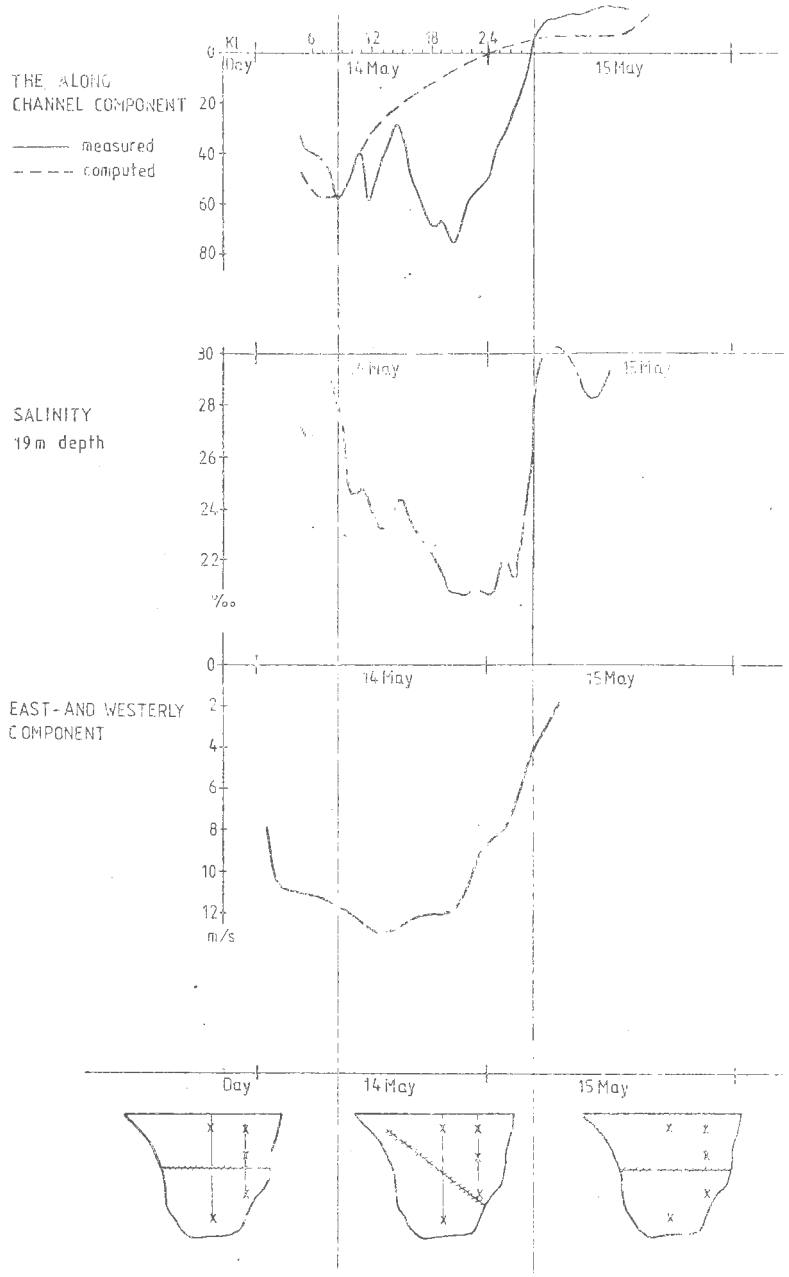


Figure 22.

The current meter at 25 m depth showed weak currents and the record has no resemblance to the computed current at 24 m which is the deepest calculated current at this station. The meter is probably placed in a semi-isolated deep with quiescent water.

The agreement between measured and computed currents at Station 5 is acceptable if on bears in mind that the computed current is a mean over the width of the channel and that the

recordings were made of the Swedish coast.

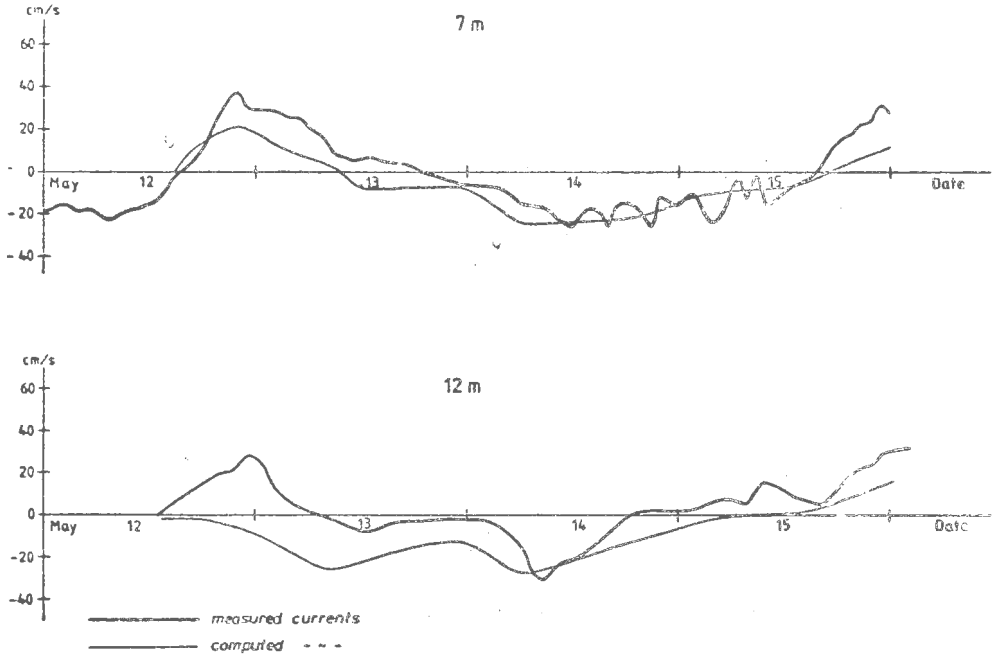


Figure 23. The currents in Station 5.

THE TUNNEL

To study the changes in the circulation caused by a tunnel connection between Helsingborg and Helsingör the bottom topography of the model was modified. Fig 24 shows a logitudinal section through the model with the tunnel. (The tunnel roof at 24 m, compare fig 15).

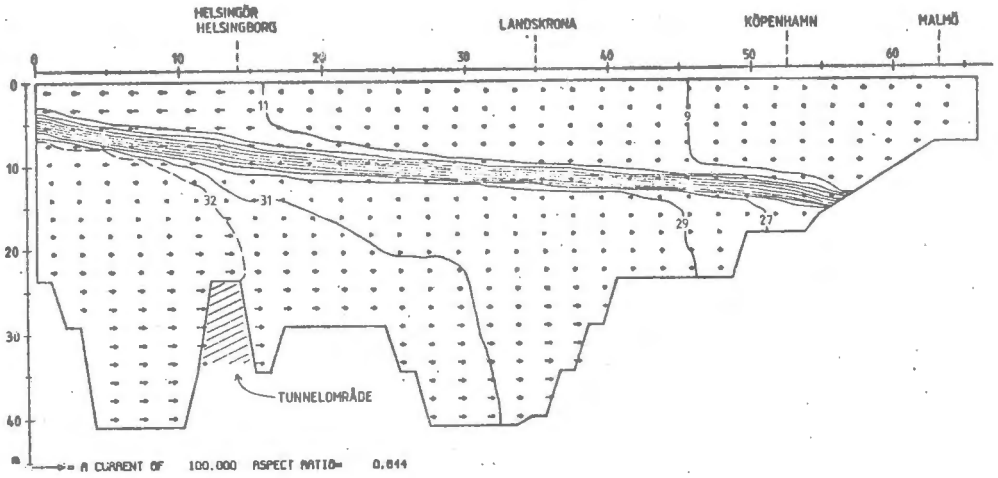


Figure 24.

The distance between the gridpoints in the horizontal is two kilometers. Two gridpoint must be used to model a tunnel which means that the tunnel in the model will be four kilometers wide. The real tunnel is planned to be only a few hundred meters wide.

The computations in the model have been carried out for the tunnel alternative which implies the smallest remaining sectional area after the construction of the tunnel. Any other alternative has not been possible to study since minor modification, less than 2 km, in the position of the tunnel, does not influence the bottom topography or sectional area of the model. The bottom friction over the four kilometer wide tunnel has been decreased in order to avoid decreasing current erroneously.

RESULT

The influence of the tunnel on the circulation has been studied with:

1. northgoing current in the surface waters; southgoing current in the deep waters.

2. southgoing current at all depths.

These situations are predominant in Öresund. In most of the cases studied, the transport through the Sound has been low (6 000 $m^3/s$). During periods with stable weather conditions the current through Öresund can be weak for several weeks and the reduction of the flow in such situations is important for the judgement of the total effect of the tunnel on Öresund. Cases with strong currents have been studied too (see paragraph "Critical flow").

The bottom friction and the turbulent mixing coefficients used were the same as in the verification runs. To get a comprehensive picture of the changes caused by the presence of a tunnel, different stratified situations were studied. The depth chosen for the main pycnocline were 10 m, 13 m and 16-17 m. The greatest effect on the intransport of deep waters is present when the pycnocline lies deep and when one current situation is succeeded by another in a never ending system. If one current situation prevails for several days the decreasing salinity inside the tunnel (increasing pressure gradient) tends to accelerate the flow. After a few days the volume flow, over the tunnel, is almost the same as it would be without the tunnel. The water coming in is, however, drawn from another depth in Kattegatt and most of the time less saline than the water transported without the tunnel.

With the tunnel roof at 24 m and the pycnocline at 16-17 m the model gives reductions of up to 40 % of the deep water transport. Periods with the pycnocline deeper than 16 m are, however, rather rare (less than 20 % of the year). The reduction of the deep water transport with a pycnocline at "normal" depth (pycnocline at 10 m) is in the model below 10 %

For the other tunnel alternative, with the tunnel roof at 28 m, the model gives reducion of 10-15 % with a deep pycnocline while it does not show any substantial reduction for cases with the pycnocline at "normal" depth.

Salinity changes slowly due to the tunnel. In a run including five days with tunnel roof at 24 m and with the pycnocline at 16-17 m depth the deep water salinity decreased 1.5 ‰. This was not a steady state value. If the run had been continued the decrease would have continued too. However, an extreme situation, with the pycnocline at great depths and with a low run off from the Baltic, is not likely to persist more than a few days. Therefore, the decrease 1.5 ‰ is a good estimate of the maximum change in salinity possible due to the tunnel.

(A more detailed treatment of the model results with the tunnel is given in (Svensson, Wilmot 1977)).

CRITICAL FLOW

When the transport in the lower layer is very big, critical flow conditions can exist where the sectional area is small. After the construction of a tunnel the critical section in the lower layer will be situated in the tunnel section. The decreased cross section caused by the tunnel will increase the number of situations with critical flow

South going current at all depth

During periods with critical flow the upper limit for the deep water transport through the tunnel section will be settled by the level of the pycnocline. The maximum transport will be less than the transport without the tunnel. A model run was carried out with an increasing water level difference between the Kattegatt and the Baltic Fig 25 shows a situation with low velocities.

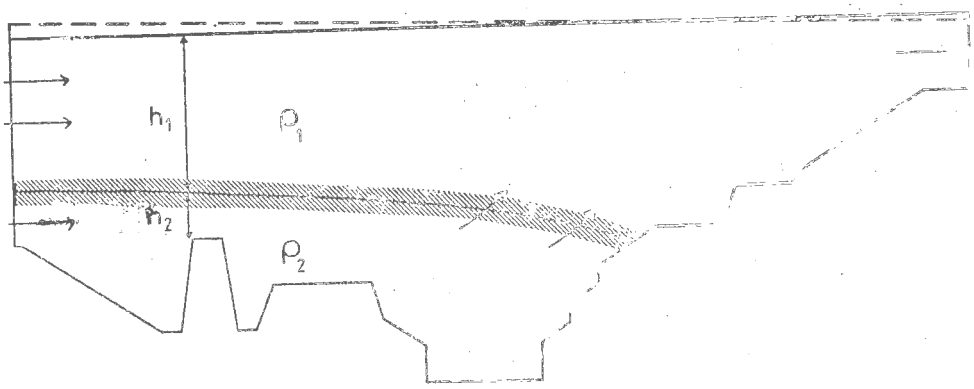


Figure 25.

If the water level difference increases, the current of the two layers also increases until the flow in the tunnel section becomes critical. The internal Froude number equals one.

$$1 = F_{I1} + F_{I2} = \frac{u_1}{\sqrt{g \frac{\Delta\rho}{\rho} h_1}} + \frac{u_2}{\sqrt{g \frac{\Delta\rho}{\rho} h_2}}$$

Where $u_1$ = velocity in the upper layer
$u_2$ = velocity in the lower layer
$h_1$ = thickness of the upper layer
$h_2$ = thickness of the lower layer

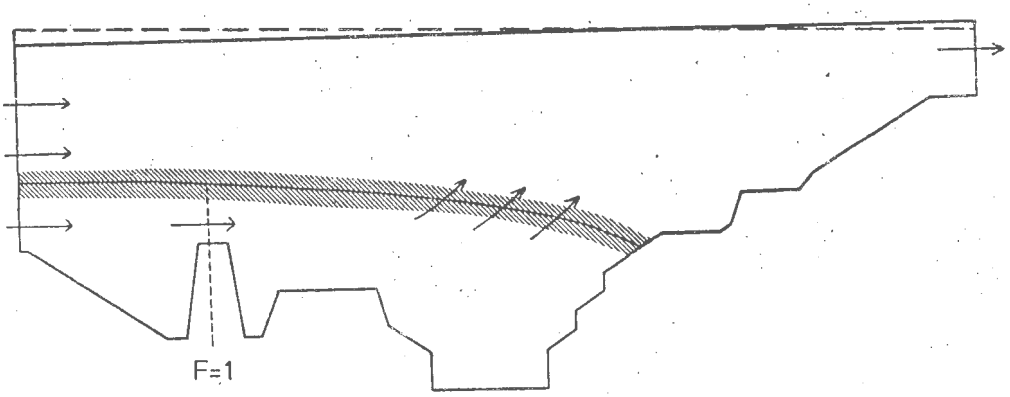


Figure 26.

When the transport is increased further, due to an increasing water level difference the pycnocline in the vincinity of the tunnel is forced to rise. The Kattegatt interface is however stationary. In this way a pressure gradient is created which constitutes the check that is significant for critical flow.

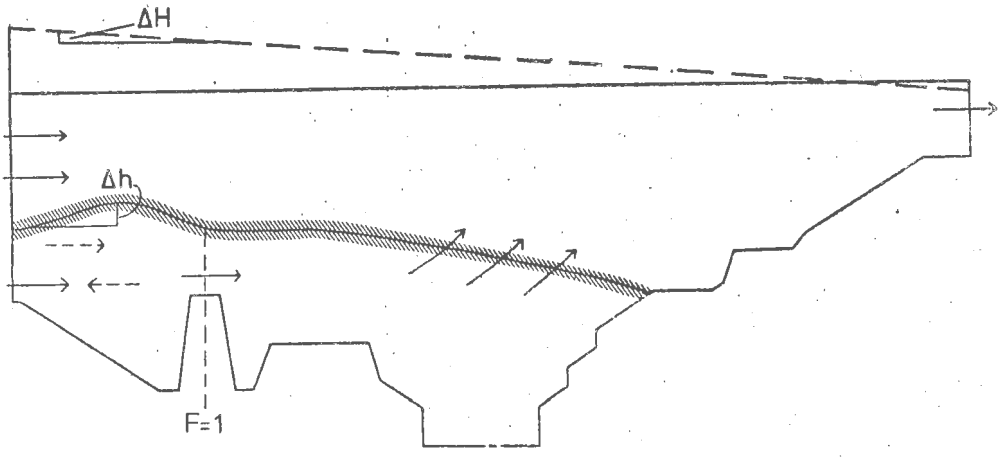


Pressure gradient due to water level differences

$\Delta P = g \cdot \rho(z) \cdot \Delta H$

Pressure gradient due to the pycnocline slope

$\Delta P = - g \cdot \Delta\rho \cdot \Delta h$

Figure 27.

The mixing behind the tunnel is not changed to any degree worth mentioning. The intransport of salt water is however increased and therefore the interface rises.

When the transport is great the pycnocline is forced to rise still more. More salt water is transported through the tunnel section but the pressure gradient working against the current is also increased.

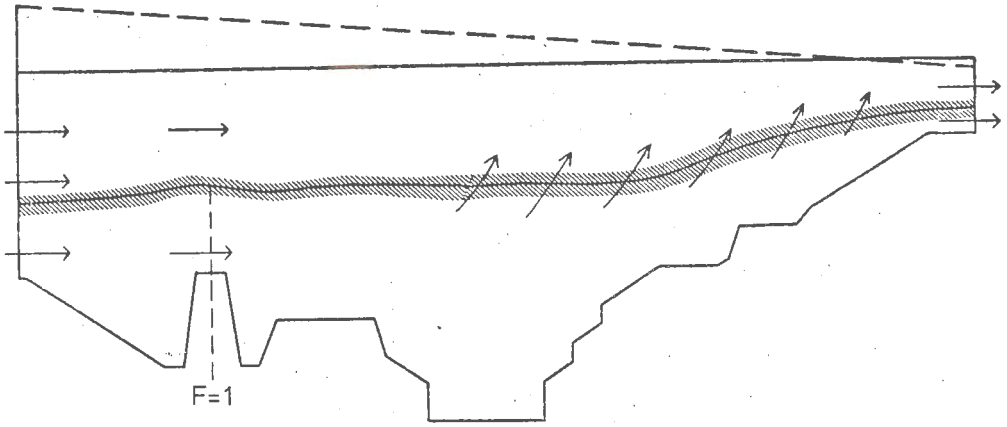


Figure 28.

The mixing behind the tunnel increases due to bigger velocities and a greater interface area available for mixing between the layers. The southgoing bottom water is partially transported over the shallow southern sill and into the Baltic.

North-going surface current; south-going bottom current

When there is a transport from the Baltic into Kattegatt the salt-water behaves like the under-current at the mouth of a river. During periods with medium transport an equilibrium develops between the salt-water transported through the interface by turbulent mixing and the water coming in over the tunnel.

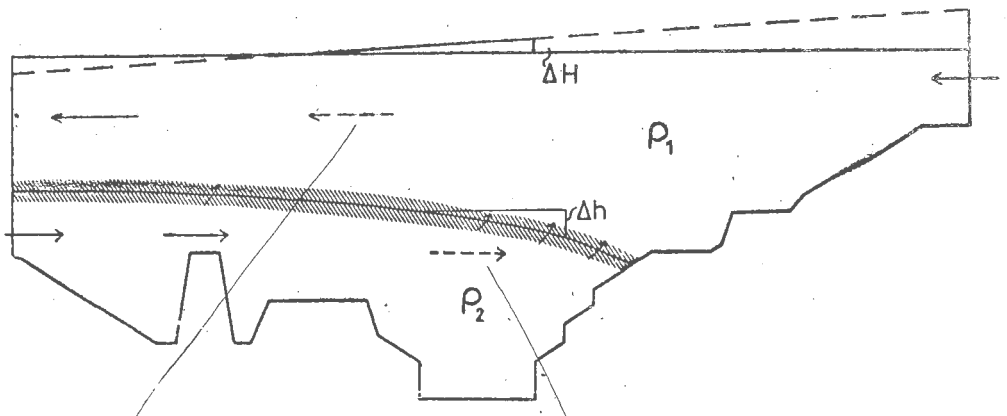


$P_1 = g \cdot \rho_1 \cdot \Delta H$ $P_2 = g\rho_1, \Delta H - g\Delta\rho \cdot \Delta h$

Figure 29.

The pressure gradient that depends on the water levels in the Baltic and the Kattegatt drives the surface water northwards. The pressure gradient in the other direction which depends on the slope of the interface preponderates in deeper layers over the force from the surface slope and forces the bottom water southwards.

If the slope of the water level and thereby the transport is big no southgoing current can persist.

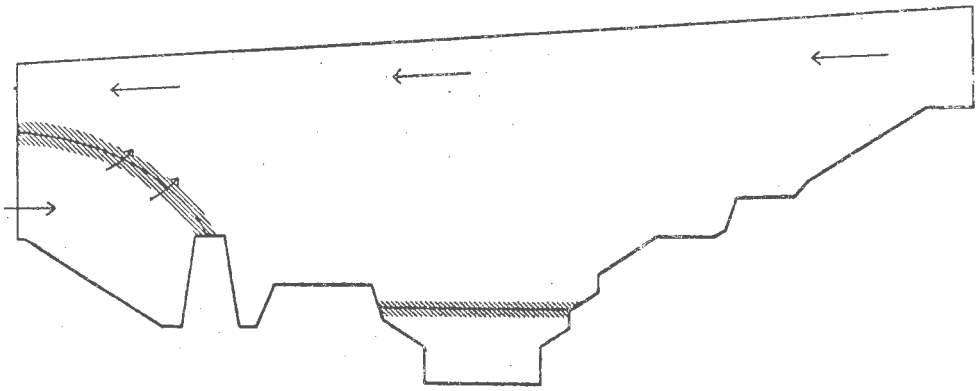

Figure 30.

Over the tunnel the deep water velocity is almost zero. There is a balance between the pressure gradient and the friction between the northgoing surface water and the bottom water.

The model shows that the current in the lower layer in an examined situation turns from southgoing to northgoing when the current in the surface layer is ≈ 80 cm/s.

In the same situation without the tunnel the current in the model was 70 cm/s in the upper layer. The intransport of deep water was 350 $m^3/s$. This is a very small transport.

The tunnel will thus reduce the southgoing transport with only a small amount in situations with strong northgoing currents in the upper layer.

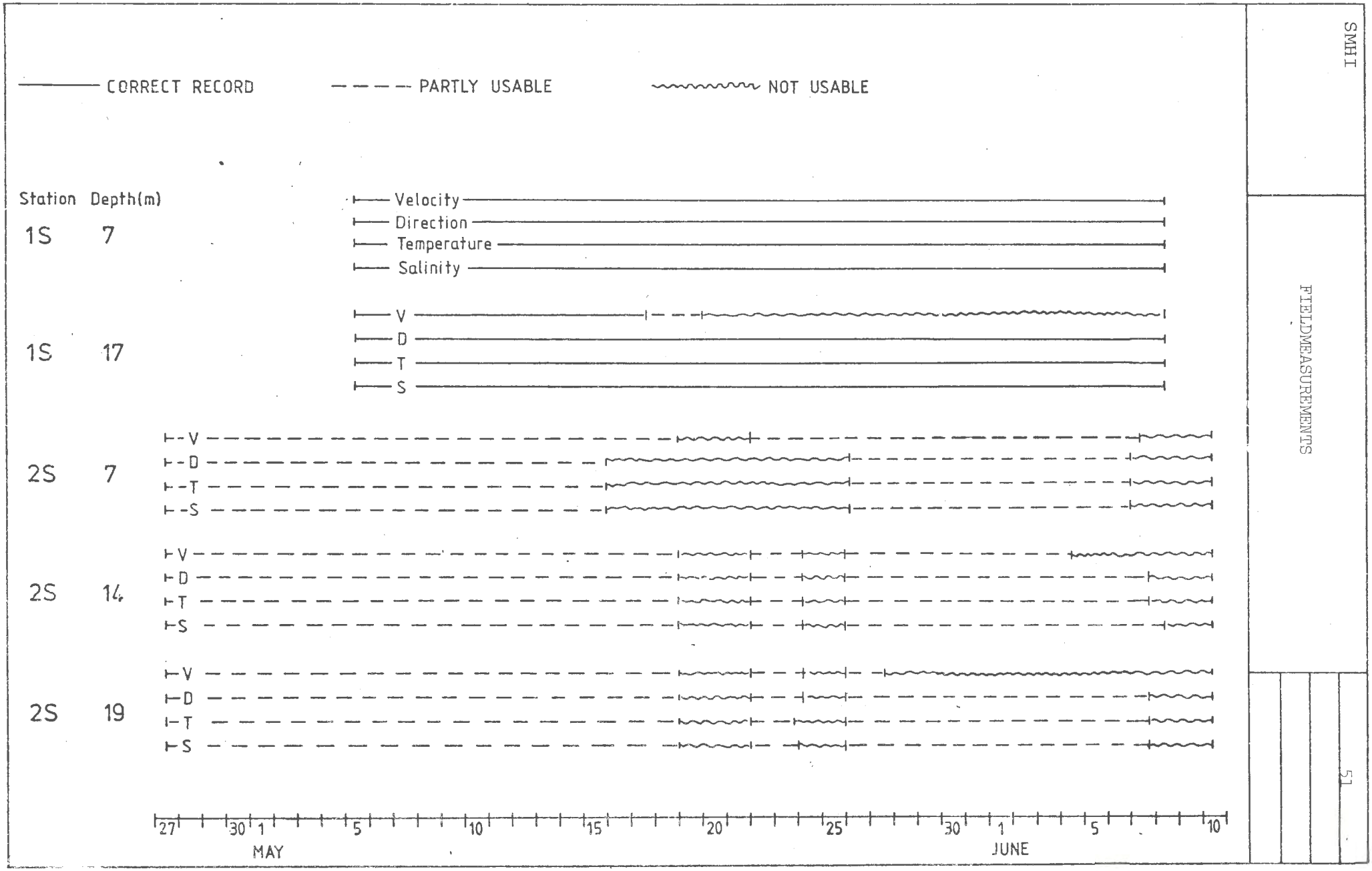
CORRECT RECORD
PARTLY USABLE
NOT USABLE
Station Depth(m)
1S 7
Velocity
Direction
Temperature
Salinity
1S 17
V
D
T
S
2S 7
2S 14
2S 19
27 30 1 5 10 15 20 25 30 1 5 10
MAY
JUNE

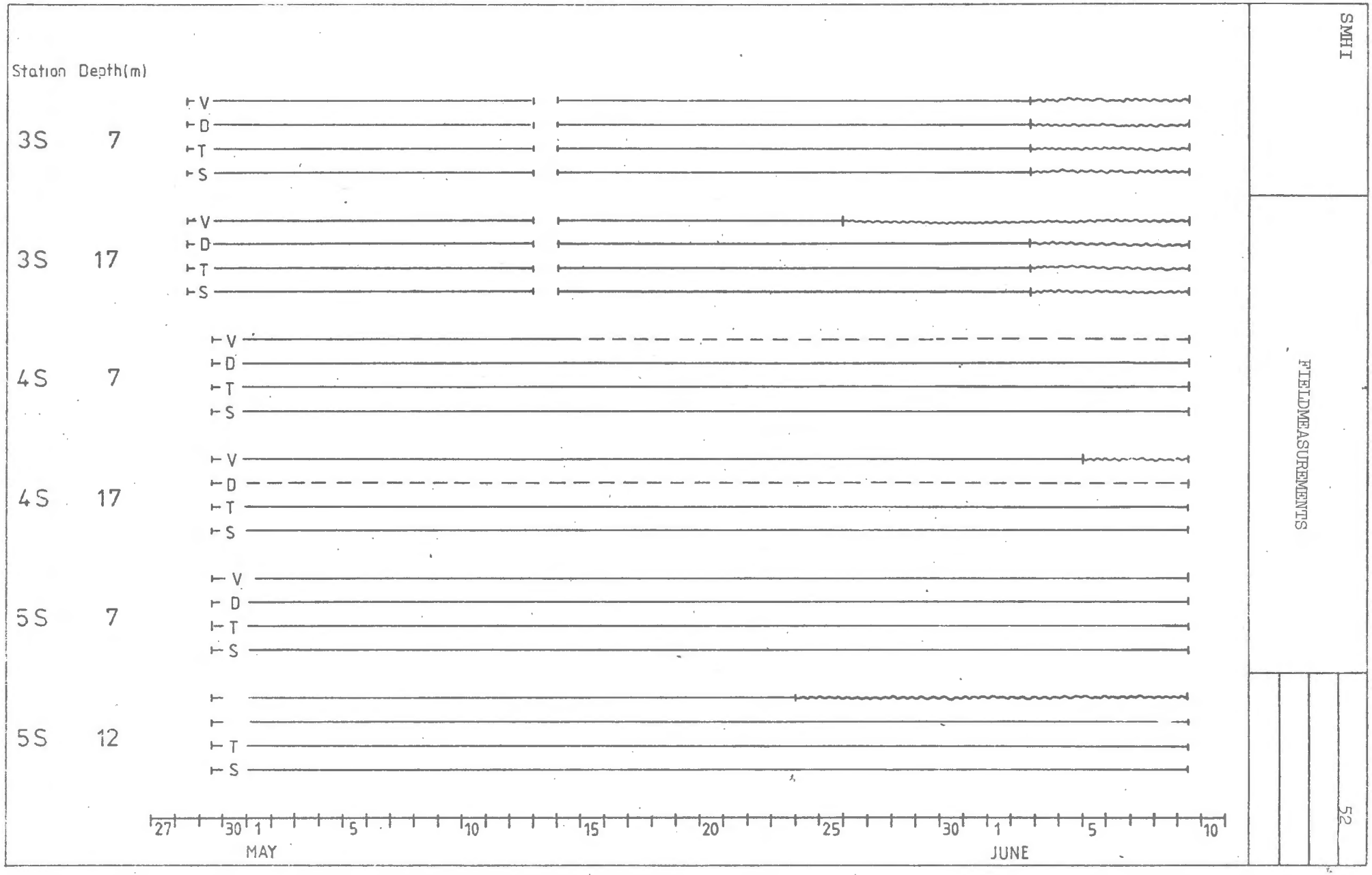
Station Depth(m)
3S 7
V
D
T
S
3S 17
V
D
T
S
4S 7
V
D
T
S
4S 17
V
D
T
S
5S 7
V
D
T
S
5S 12
T
S
27 30 1 5 10 15 20 25 30 1 5 10
MAY
JUNE

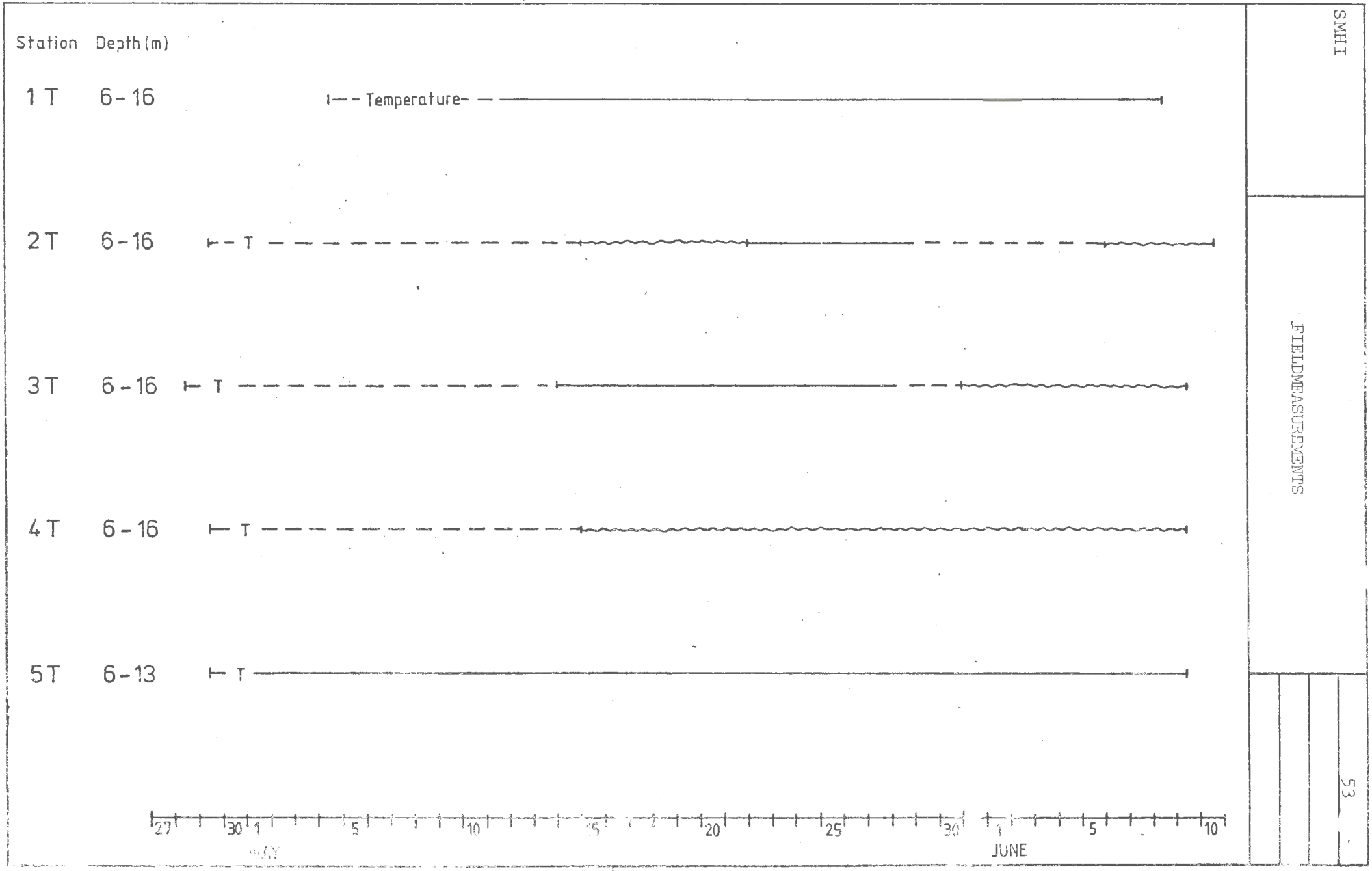
Station Depth (m)
1 T 6-16
Temperature
2 T 6-16
T
3 T 6-16
T
4 T 6-16
T
5 T 6-13
T
27 30 1 5 10 15 20 25 30 1 5 10
MAY
JUNE

REFERENCES

Arakawa, A. (1966): Computational design for long-term numerical integration of the equations of fluid motion: I. Two-dimensional incompressible flow, J. of Comp. Physics, Vol. 1, No. 1, pp. 392-405

Blumberg, A.F. (1977): Numerical model of estuarine circulation, J. of the hydraulics division, Proc. of the ASCE, Vol. 103, No. HY 3

Fisher, G. (1965): A survey of finite-difference approximations to the primitive equations, Mon. Weather Rev., Vol. 93, No. 1, pp. 1-10

Fredrich, H., Levitus, S. (1972): An approximation to the equations of state for sea water, suitable for numerical ocean models, J. of Ph. Oceanography, Vol. 2, No. 4

Grammeltvedt, A. (1969): A survey of finite-difference schemes for the primitive equations for a barotropic fluid, Mon. Weather Rev., Vol. 97, No. 5, pp. 384-404

Kullenberg, G. (1976): On vertical mixing and the energy transfer from the wind to the water, Tellus, Vol. 28, No. 2

Kurihara, Y. (1965): On the use of implicit and iterative methods for the time integration of the wave equation, Mon. Weather Rev., Vol. 93, No. 1, pp. 33-46

Lilly, D.K. (1965): On the computational stability of numerical solutions of time-dependent non-linear geophysical fluid dynamics problems, Mon. Weather Rev., Vol. 93, No. 1, pp. 11-26

Ogura, Y., Yagihashi,A. (1969): A numerical studey of convection rolls in a flow between horizontal parallel plates, J. of the Met. Soc. of Japan, Vol. 47, No. 3, pp. 205-217

Piacsek, S.A., Williams, G.P. (1970): Conservation properties of convection difference schemes, J. of Comp. Phys., Vol. 6, pp. 392-405

Pritchard, D.W. (1956): The dynamic structure of a coastal plain estuary, J. Marine Res., Vol. 15, pp 33-42

---- (1958): The equations of mass continuity and salt continuity in estuaries, J. Marine Res., Vol. 17, pp. 412-423

Shuman, F.G. (1962): Numerical experiments with the primitive equations, Proceedings of the International Symposium on Numerical Weather Prediction in Tokyo, November 1960, Meteorological Society of Japan, Tokyo, Mar. 1962, pp. 85-107

Stewart, R.W. (1957): A note on the dynamic balance for estuarine circulation, J. Marine Res., Vol. 16, pp. 34-39

Svansson, A., Szaron, J. (1975): Sea level computations of the Baltic with a 20-canal model. Tellus, Vol. 27, No. 6

Wilmot,W. (1976): A numerical model of the effects of reactor cooling water on fjord circulation I and II, SMHI Rapporter HYDROLOGI OCH OCEANOGRAFI Nr RHO 6

Young, J.A. (1968): Coparative properties of som time differencing schemes for linear and nonlinear oscillations, Mon. Weather Rev., Vol. 96, No. 6, pp. 357-364

Notiser och preliminära rapporter

Serie HYDROLOGI

Nr 1 Sundberg-Falkenmark M
Om isbärighet. Stockholm 1963

Nr 2 Forsman, A
Snösmältning och avrinning. Stockholm 1963

Nr 3 Karström, U
Infrarödteknik i hydrologisk tillämpning: Värmebilder som hjälpmedel i recipientundersökningar. Stockholm 1966

Nr 4 Moberg, A
Svenska sjöars isläggnings- och islossningstidpunkter 1911/12-1960/61. Del 1. Redovisning av observationsmaterial. Stockholm 1967

Nr 5 Ehlin, U & Nyberg, L
Hydrografiska undersökningar i Nordmalingsfjärden. Stockholm 1968

Nr 6 Milanov, T
Avkylningsproblem i recipienter vid utsläpp av kylvatten. Stockholm 1969

Nr 7 Ehlin, U & Zachrisson, G
Spridningen i Vänerns nordvästra del av suspenderat materiel från skredet i Norsälven i april 1969. Stockholm 1969

Nr 8 Ehlert, K
Mälarens hydrologi och inverkan på denna av alternativa vattenavledningar från Mälaren. Stockholm 1970

Nr 9 Ehlin, U & Carlsson, B
Hydrologiska observationer i Vänern 1959-1968 jämte sammanfattande synpunkter. Stockholm 1970

Nr 10 Ehlin, U & Carlsson, B
Hydrologiska observationer i Vänern 17-21 mars 1969. Stockholm 1970

Nr 11 Milanov, T
Termisk spridning av kylvattenutsläpp från Karlshamnsverket. Stockholm 1971

Nr 12 Persson, M
Hydrologiska undersökningar i Lappträskets representativa område. Rapport I. Stockholm 1971

Nr 13 Persson, M
Hydrologiska undersökningar i Lappträskets representativa område. Rapport II. Snömätningar med snörör och snökuddar Stockholm 1971

Nr 14 Hedin, L
Hydrologiska undersökningar i Velens representativa område. Beskrivning av området, utförda mätningar samt preliminära resultat. Rapport I. Stockholm 1971

Nr 15 Forsman, A & Milanov, T
Hydrologiska undersökningar i Velens representativa område.
Markvattenstudier i Velenområdet. Rapport II. Stockholm 1971

Nr 16 Hedin, L
Hydrologiska undersökningar i Kassjöåns representativa område.
Nederbördens höjdberoende samt kortfattad beskrivning av området. Rapport I. Stockholm 1971

Nr 17 Bergström, S & Ehlert, K
Stochastic Streamflow Syntheses at the Velen representative Basin. Stockholm 1971

Nr 18 Berström, S
Snösmältningen i Lappträskets representativa område som funktion av lufttemperaturen. Stockholm 1972

Nr 19 Holmström, H
Test of two automatic water quality monitors under field conditions. Stockholm 1972

Nr 20 Wennerberg, G
Yttemperaturkartering med strålningstermometer från flygplan över Vänern under 1971. Stockholm 1972

Nr 21 Prych, A
A warm water effluent analyzed as a buoyant surface jet.
Stockholm 1972

Nr 22 Bergström, S
Utveckling och tillämpning av en digital avrinningsmodell.
Stockholm 1972

Nr 23 Melander, O
Beskrivning till jordartskarta över Lappträskets representativa område. Stockholm 1972

Nr 24 Persson, M
Hydrologiska undersökningar i Lappträskets representativa område. Rapport III. Avdunstning och vattenomsättning.
Stockholm 1972

Nr 25 Häggström, M
Hydrologiska undersökningar i Velens representativa område.
Rapport III. Undersökning av torrperioderna under IHD-åren fram t o m 1971. Stockholm 1972

Nr 26 Bergström, S
The application of a simple rainfall-runoff model to a catchment with incomplete data coverage. Stockholm 1972

Nr 27 Wändahl, T & Bergstrand, E
Oceanografiska förhållanden i svenska kustvatten.
Stockholm 1973

Nr 28 Ehlin, U
Kylvattenutsläpp i sjöar och hav. Stockholm 1973

Nr 29 Andersson, U-M & Waldenström, A
Mark- och grundvattenstudier i Kassjöåns representativa område. Stockholm 1973

Nr 30 Milanov, T
Hydrologiska undersökningar i Kassjöåns representativa område.
Markvattenstudier i Kassjöåns område. Rapport II. Stockholm 1973

SMHI Rapporter

HYDROLOGI OCH OCEANOGRAFI

Nr RHO 1 — Wahl, J C
Verification of heated water jet numerical model
Stockholm 1974

Nr RHO 2 — Svensson, J
Calculation of poison concentrations from a hypothetical accident off the Swedish coast
Stockholm 1974

Nr RHO 3 — Vasseur, B
Temperaturförhållanden i svenska kustvatten
Stockholm 1975

Nr RHO 4 — Svensson, J
Beräkning av effektiv vattentransport genom Sunninge sund till Byfjorden
Stockholm 1975

Nr RHO 5 — Bergström, S & Jönsson, S
The application of the HBV runoff model to the Filefjell research basin
Norrköping 1976

Nr RHO 6 — Wilmot, W
A numerical model of the effects of reactor cooling water on fjord circulation
Norrköping 1976

Nr RHO 7 — Bergström, S
Development and Appl. of a Conceptual Runoff Model
Norrköping 1976

Nr RHO 8 — Svensson, J
Seminars at SMHI 1976-03-29--04-01 on Numerical Models of the Spreading of Cooling-water
Norrköping 1976

Nr RHO 9 — Simons, J & Funkquist, L & Svensson, J
Application of a numerical model to Lake Vänern
Norrköping 1977

Nr RHO 10 — Svensson, S
A statistical study for automatic calibration of a conceptual runoff model
Norrköping 1977

Nr RHO 11 — Bork, I
Model studies of dispersion of pollutants in Lake Vänern
Norrköping 1977

Nr RHO 12 — Fremling, S
Sjöisars beroende av väder och vind, snö och vatten
Norrköping 1977

SMHI Rapporter

HYDROLOGI OCH OCEANOGRAFI

Nr RHO 13 Fremling, S
Sjöisars bärighet vid trafik.
Norrköping 1977

Nr RHO 14 Bork, I
Preliminary model studies of sinking plumes.
Norrköping 1978

Nr RHO 15 Svensson, J & Wilmot, W
A numerical model of the circulation in Öresund. Evaluation of the effect of a tunnel between Helsingborg and Helsingör.
Norrköping 1978